

Comparison of two combinatorial models of global network dynamics

Peter Crawford-Kahrl, Bree Cummins, Tomas Gedeon

November 25, 2021

Abstract

Modeling the dynamics of biological networks introduces many challenges, among them the lack of first principle models, the size of the networks, and difficulties with parameterization. Discrete time Boolean networks and related continuous time switching systems provide a computationally accessible way to translate the structure of the network to predictions about the dynamics. Recent work has shown that the parameterized dynamics of switching systems can be captured by a combinatorial object, called a DSGRN database, that consists of a parameter graph characterizing a finite parameter space decomposition, whose nodes are assigned a Morse graph that captures global dynamics for all corresponding parameters.

We show that for a given network there is a way to associate the same type of object by considering a continuous time ODE system with a continuous right-hand side, which we call an L-system. The main goal of this paper is to compare the two DSGRN databases for the same network. Since the L-systems can be thought of as perturbations (not necessarily small) of the switching systems, our results address the correspondence between global parameterized dynamics of switching systems and their perturbations. We show that, at corresponding parameters, there is an order preserving map from the Morse graph of the switching system to that of the L-system that is surjective on the set of attractors and bijective on the set of fixed point attractors. We provide important examples showing why this correspondence cannot be strengthened.

1 Introduction

Nonlinear dynamics is notoriously difficult. Since a complete rigorous analysis of dynamics of nonlinear systems of coupled differential equations of dimension higher than two is almost impossible, any interrogation of higher dimensional systems of ODE usually relies on numerical simulations.

In problems arising in cellular biology, there is a need to model many mutually interacting types of molecules that together control cellular fate. Incorrectly functioning genetic and regulatory networks are at the core of cancer, diabetes, and other systemic diseases [9, 11, 27]. The crucial importance of these networks for cell biology and human health makes

development of effective methods that can characterize dynamics supported by a network over all parameters a high priority [1, 3, 23, 2, 25, 26, 28]. In the context of cell biology, the problems of nonlinear dynamics are compounded by the lack of first principles that would determine appropriate nonlinearities, the difficulty in obtaining precise experimental data needed to determine parameters, and the need to analyze the dynamics of 5-10 dimensional systems over 30-50 parameters.

Recently, we introduced in [12, 13] a new approach to this problem that assigns two finite objects to any network with positive and negative edges. First is a *parameter graph* whose nodes are in 1-1 correspondence with regions in the parameter space, where these regions form a decomposition of the parameter space. To each domain of the parameter space, i.e. a node of the parameter graph, there is an associated *state transition graph* that characterizes allowable transitions between well-defined states of the phase space. Since state transition graphs can be large, a useful description of the recurrent trajectories is a *Morse graph*, which is graph of strongly connected path components of the state transition graph. The entire structure, where to each node of the parameter graph there is an associated Morse graph that captures recurrent dynamics valid for all parameters in the corresponding parameter region, is called Database of Signatures Generated by Regulatory Networks (DSGRN).

The advantages of such a description of global dynamics is its finiteness and the resulting computability; yet this description, which inevitably must be coarser than the traditional concepts of dynamical systems theory, allows searching the database for parameters that support dynamics like bistability, hysteresis, non-constant recurrent behavior, and the ability to compare the prevalence of such signatures across multiple networks.

The development of DSGRN was guided by work over the last two decades on *switching systems* [20, 31, 32, 8, 14, 15] which are ordinary differential equations with piecewise constant nonlinearities. The value of each nonlinearity changes discontinuously when an argument crosses a threshold. The collection of these thresholds divides the phase space into domains, which form the nodes of the state transition graph. The choice of piecewise constant nonlinearities presents two sets of challenges. The mathematical challenge is to make sense of the continuation of solutions that enter the intersection of multiple thresholds. The biological challenge is to justify the selection of piecewise constant nonlinearities as appropriate models of biological processes. Our view is that DSGRN, being by its construction a finite, computable and robust object, gives us information not only about the switching system that was used to construct it, but it also describes all nearby continuous systems [18].

There has been a considerable interest in the computational biological systems community in trying to enlarge a class of ODE systems for which finite state transition graphs capture the behavior of all solutions [5, 7, 4, 6]. The result of these papers show how to construct a phase transition graph for so called multi-affine systems, where nonlinearities are piecewise linear functions.

In this paper we generalize their result to nonlinearities that are step functions with Lipschitz continuous bridges, which we call L-functions. These functions have alternating intervals where the function is constant, and the intervals where function is Lipschitz and bounded between the (constant) values of the function on neighboring intervals. We show that the

dynamics of such systems are captured by a state transition graph, and consequently one can associate DSGRN results to a network based on interactions mediated by L-functions. The central question that we address in this paper is relationship between global dynamics of two sets of models, as captured by DSGRN description. Given a regulatory network, we can associate to it two different DSGRN databases characterizing global dynamics across all parameters: one based on a switching system description, and the other based on L-functions. A natural question is how these two objects are related. This is a global version of a question that has been investigated before where a piecewise constant nonlinearity is perturbed around a threshold to form a continuous function [14, 24, 18].

We begin by introducing a general framework for the construction of state transition graphs. This framework encompasses the well-known case of Boolean maps [30, 31, 32, 10, 29], and extends it to a *multi-level discrete map* D , which increases the number of discrete states available to each node in the network [17, 21]. We then introduce the idea of a *nearest neighbor multi-valued map* \mathcal{F} , which may arise as an *asynchronous update rule* of D in a way analogous to that discussed in [10] for a Boolean model. \mathcal{F} obeys an adjacency condition which allows only one node of the network to change its state at a time.

We then formally introduce S-systems (switching systems) and L-systems (ODE systems based on L-functions), and demonstrate the relationship between maps D , \mathcal{F} , and these ODE systems. We show that there is a map between the parameters of the S- and L-systems, and that under this map, there is a well-defined relationship between the Morse graphs of the two systems. In particular, the map from the S-system Morse graph to the L-system Morse graph is bijective on fixed points, surjective on attractors, and order-preserving otherwise. We conclude with a series of examples that demonstrate that these relationships cannot be strengthened.

2 General System

Definition 2.1. A *regulatory network* $\mathbf{RN} = (V, E)$ is a graph with network nodes $V = \{1, 2, \dots, N\}$ and signed, directed edges $E \subset V \times V \times \{\rightarrow, \vdash\}$. For $i, j \in V$, we will use the notation $(i, j) \in E$ to denote a directed edge from i to j of either sign, $i \rightarrow j$ to denote an *activation* or positive interaction, and $i \vdash j$ to denote a *repression* or negative interaction. We only consider regulatory networks with no negative self-regulation, $i \vdash i$.

We define the *targets* of a node i as

$$\mathbf{T}(i) := \{j \mid (i, j) \in E\}$$

and the *sources* of a node i as

$$\mathbf{S}(i) := \{j \mid (j, i) \in E\}$$

We exclude networks with negative self-regulation because they present technical difficulties in switching systems; see [16] for an excellent set of references. In many cases, negative

self-regulation can be replaced in a model by an intermediate node [16, 22] which obviates the need for a negative self-edge in a regulatory network.

As an example regulatory network **RN** we consider $\{x \dashv y, y \dashv x\}$. Here each node has as a target the other node.



Figure 1: Two dimensional example **RN**.

One way to associate dynamics to a network is to construct a Boolean net [30, 31, 32, 10, 29]. Each node can attain values 0 or 1 that are interpreted as low and high levels of activity. At each node i with $|\mathbf{S}(i)| = n$, there is an associated local Boolean function that assigns to each of the 2^n input binary sequences a value of $x_i \in \{0, 1\}$. The collection of the local Boolean functions over the network forms a Boolean function $B : \{0, 1\}^N \rightarrow \{0, 1\}^N$, that acts on a space of binary sequences of length N . Iterations B^r of this function model long-term behavior of the network. The collection of all local Boolean functions that can be selected at each node parameterize the set of all Boolean functions $\mathcal{B}_{\mathbf{RN}} = \{B\}$ compatible with the given network **RN**. Since both the domain $\{0, 1\}^N$ of B and this parameterization of $\mathcal{B}_{\mathbf{RN}}$ are discrete sets, there is no concept of a “small” perturbation from one Boolean function to another.

Motivated by this example, we now propose a different way to associate to a network a dynamical system on a finite state space. These dynamical systems will be parameterized by a continuous parameter space, and so it makes sense to ask how these finite dynamical systems behave under perturbations. Even though parameter space is continuous, we will show that it can be divided into a finite number of regions where the behavior of the dynamics is the same, enabling a global description of the network over all real-valued parameters.

We start by assuming that to each node of the network there is an associated variable $x_i \in [0, \infty)$, which represents the concentration of chemical species i . We assume that there are finite number of thresholds $\theta_{1,i}, \dots, \theta_{m_i,i}$ that divide the semi-axis $[0, \infty)$ to $m_i + 1$ intervals I_k . The effect of node i on its target nodes $j \in \mathbf{T}(i)$ will only depend on the interval I_k with $x_i \in I_k$ and not on the particular value x_i . The collection of thresholds $\{\theta_{j,i}\}$ partitions $[0, \infty)^N$ into a finite number of domains κ , characterized by the property that the projection on i -th variable $\pi_i(\kappa) = I_k$ for a unique $k \in \{0, \dots, m_i\}$ for every i . We let $x = (x_1, \dots, x_N)$ denote a point in $[0, \infty)^N$.

Definition 2.2. Let $\mathcal{V}(i) := \{0, \dots, m_i\}$ and let

$$G_i : [0, \infty) \rightarrow \mathcal{V}(i) \tag{1}$$

be a *state function* defined by $G_i(x_i) = k$ if and only if $x_i \in I_k$. Let $\mathcal{V} = \prod_i \mathcal{V}(i)$ be the set of all *states* of the network **RN** and let

$$G : [0, \infty)^N \rightarrow \mathcal{V}$$

be the vector-valued function with coordinate functions G_i . For a given domain κ , the value $G(x)$ does not depend on $x \in \kappa$. Therefore we can assign the *state* $s := G(x) \in \mathcal{V}$, $x \in \kappa$ to the domain κ , and we will write $s = g(\kappa)$. Viewed as a map on the set of domains $\mathcal{K} = \{\kappa\}$ in $[0, \infty)^N$, g is a bijection between domains κ and states $s \in \mathcal{V}$

$$g : \mathcal{K} \longrightarrow \mathcal{V}. \quad (2)$$

We postulate that along each edge (i, j) in the network a signal from the node i to the node j can be transmitted, and this signal attains only finite number of values $A_{j,i} := \{a_{j,i}^1 < \dots < a_{j,i}^t\}$. This transmission is characterized via a function

$$F_{j,i} : \mathcal{V}(i) \rightarrow A_{j,i} \quad (3)$$

that only depends on the state $k \in \mathcal{V}(i)$ of x_i . Let $A = \prod A_{j,i}$ be a product of all sets $A_{j,i}$ and let

$$F : \mathcal{V} \rightarrow A$$

be the vector-valued function with coordinate functions $F_{j,i}$.

A final piece of our description of discrete dynamics on a network **RN** is a collection of functions M_i , one for each node i of the network,

$$M_i : \prod_{j=1}^{|\mathbf{S}(i)|} A_{i,j} \rightarrow [0, \infty) \quad (4)$$

that take the values that are being transmitted along the edges leading into i and produce the values x_i . Let M be the vector-valued function with coordinate functions M_i ,

$$M : A \rightarrow [0, \infty)^N.$$

The composition

$$D := G \circ M \circ F : \mathcal{V} \rightarrow \mathcal{V} \quad (5)$$

is a generalization of the Boolean function B , called a *multi-level discrete function* [17, 21].

The set of values A in Definition 2.2 replaces the binary values 0, 1 that are transmitted in a Boolean network. Note that even when two outward edges from node i have the same sign, say $i \rightarrow j$ and $i \rightarrow l$, different values can be transmitted to j and l since the values $F_{j,i}(k)$ and $F_{l,i}(k)$ may be different. This generalizes the behavior of a traditional Boolean function.

One serious objection to representing the dynamics of a network by either a Boolean function B or a discrete function D is that it does not respect the continuity of the underlying biological process. In particular, the Boolean vector $(B(s) - s)$ can be non-zero in more than one component which implies that two or more processes switch at exactly the same time. In addition, the vector $(D(s) - s)$ can have entries greater than 1 in absolute value, which clearly violates continuity of the underlying chemical process. An *asynchronous update* of Boolean function B has been proposed [10, 33] to generate dynamics that are compatible continuous variables, and we extend this approach to map D .

For a given multi-level discrete map D we define a *nearest neighbor multi-valued map* \mathcal{F} , that will only allow transitions from domains to the adjacent domains in phase space, where these transitions are induced by D .

Definition 2.3. Let s_1 and s_2 be the states of two domains κ_1 and κ_2 , $s_1 = g(\kappa_1)$ and $s_2 = g(\kappa_2)$ from (2). These domains are adjacent along i (and so are the states) if and only if there exists exactly one index i such that

$$\pi_i(\kappa_1) \cap \pi_i(\kappa_2) \subset \{x_i = \theta_{j,i}\} \text{ and } \pi_j(\kappa_1) = \pi_j(\kappa_2) \text{ for all } j \neq i.$$

Let $t_1 = D(s_1)$. The *asynchronous update rule* of D is a nearest neighbor multi-valued map $\mathcal{F} : \mathcal{V} \rightrightarrows \mathcal{V}$, such that $s_2 \in \mathcal{F}(s_1)$ if and only if

- (a) $s_1 = t_1 = s_2$; or
- (b) $t_1 \neq s_1$, $s_1 := (s_{1,1}, s_{1,2}, \dots, s_{1,N})$ and $s_2 := (s_{2,1}, s_{2,2}, \dots, s_{2,N})$ are adjacent along i and either
 1. $s_{1,i} < s_{2,i} \leq t_{1,i}$ or
 2. $s_{1,i} > s_{2,i} \geq t_{1,i}$.

\mathcal{F} is sometimes represented as a graph, called a *state transition graph*, $(\mathcal{V}, \mathcal{E})$, where $(s, t) \in \mathcal{E}$ if and only if $t \in \mathcal{F}(s)$.

We note that nearest neighbor multi-valued maps \mathcal{F} can be constructed without reference to an underlying multi-level discrete map D by considering an arbitrary multi-valued map $\mathcal{F} : \mathcal{V} \rightrightarrows \mathcal{V}$ where the image $\mathcal{F}(s)$ is adjacent to s .

Since the number of states in \mathcal{V} can be very large, the dynamics of iterates of \mathcal{F} can be captured by a more compact representation [33, 12].

Definition 2.4. A *recurrent component* of the map \mathcal{F} is a *strongly connected path component* of the associated graph $(\mathcal{V}, \mathcal{E})$. In other words, it is a maximal collection of vertices $\mathcal{C} \subset \mathcal{V}$ such that for any $u, v \in \mathcal{C}$ there exists a non-empty path from u to v with vertices in \mathcal{C} and edges in \mathcal{E} . In the context of dynamical systems we refer to a recurrent component of \mathcal{F} as a *Morse set* of \mathcal{F} and denote it by $\mathcal{M} \subset \mathcal{V}$. The collection of all recurrent components of \mathcal{F} is denoted by

$$\text{MD}(\mathcal{F}) := \{\mathcal{M}(p) \subset \mathcal{V} \mid p \in \mathbf{P}\}$$

and is called a *Morse decomposition* of \mathcal{F} , where \mathbf{P} is an index set. Recurrent components inherit a well-defined partial order by the reachability relation in the directed graph $(\mathcal{V}, \mathcal{E})$. Specifically, we may write the partial order on the indexing set \mathbf{P} of $\text{MD}(\mathcal{F})$ by defining

$$q \leq p \quad \text{if there exists a path in } (\mathcal{V}, \mathcal{E}) \text{ from an element of } \mathcal{M}(p) \text{ to an element of } \mathcal{M}(q).$$

Definition 2.5. The *Morse graph* of \mathcal{F} , denoted $\text{MG}(\mathcal{F})$, is the Hasse diagram of the poset (\mathbf{P}, \leq) . We refer to the elements of \mathbf{P} as the *Morse nodes* of the graph.

An intriguing question is the characterization of the set of ordinary differential equations models that are compatible with a given map \mathcal{F} . This class of equation will share the same broad dynamical features that are captured by the Morse graph of \mathcal{F} . In the other direction, identifying a map \mathcal{F} for a given ODE system would facilitate its analysis, because of the inherent computability of the Morse graph from the map \mathcal{F} .

Definition 2.6. We say an ordinary differential equation model with variables x_i is *compatible* with a nearest neighbor multi-valued map \mathcal{F} if solutions $x(t)$ can traverse from domain κ_1 to adjacent domain κ_2 only if $s_2 \in \mathcal{F}(s_1)$.

In this manuscript, we offer two examples of ordinary differential equation models associated to a regulatory network that are compatible with a nearest neighbor map \mathcal{F} , which we call S-systems and L-systems. The S-system, also known as a switching system in the literature, has been very well studied, while the ability to define \mathcal{F} associated to the L-system is a new contribution. In both cases, the association between the continuous ODE system and a discrete map \mathcal{F} allows us to combine the best features of both worlds. On one hand, there is a combinatorial representation of both the dynamics and the parameters, which allows computational enumeration of all types of dynamics for all parameters. On the other hand, the underlying assumptions of continuity allow us to interpret the dynamics of iterates of \mathcal{F} in terms of solutions of systems of ordinary differential equations.

2.1 S-system

Given a regulatory network $\mathbf{RN} = (V, E)$, to each node i we assign a parameter γ_i^S , which will be interpreted as a rate of degradation of x_i . For each edge $(i, j) \in E$ we associate three numbers: a threshold $\theta_{j,i}$ and a low value $l_{j,i}^S$ and a high value $u_{j,i}^S$, so that $A_{j,i} = \{l_{j,i}^S, u_{j,i}^S\}$ (see Definition 2.2). We require for all i that

$$0 < \gamma_i^S, \quad 0 < l_{j,i}^S < u_{j,i}^S, \quad 0 < \theta_{j,i}, \quad \theta_{j,i} \neq \theta_{k,i} \text{ whenever } j \neq k$$

and we call an *S-parameter* of \mathbf{RN} the tuple $z^S = (l^S, u^S, \theta, \gamma^S) \in \mathbb{R}^{d^S}$ where $d^S = \#(V) + 3\#(E)$. The collection of the threshold parameters $\{\theta_{j,i}\}$ partitions $[0, \infty)^N$, which facilitates the definition of the function $G^S : [0, \infty)^N \rightarrow \mathcal{V}^S$, $\mathcal{V}^S = \prod_i \mathcal{V}(i)$, via its component functions

$$G_i^S : [0, \infty) \setminus \{\theta_{j,i}\} \rightarrow \mathcal{V}(i) = \{0, \dots, |\mathbf{T}(i)|\}$$

as in Definition 2.2. Let $\theta_{j,i}(k)$ be k -th threshold in the linearly ordered set $\{\theta_{\ell,i} : \ell \in \mathbf{T}(i)\} \subset [0, \infty)$. Then the function G_i^S is defined by

$$x_i < \theta_{j,i} \Leftrightarrow G_i^S(x_i) \leq k - 1; \quad x_i > \theta_{j,i} \Leftrightarrow G_i^S(x_i) > k - 1.$$

We define $F_{j,i}^S$ from (3) as

$$F_{j,i}^S \circ G_i^S(x_i) := \begin{cases} l_{j,i}^S & \text{if } G_i^S(x_i) \leq k - 1 \text{ and } i \rightarrow j, \text{ or } G_i^S(x_i) > k - 1 \text{ and } i \dashv j \\ u_{j,i}^S & \text{for } G_i^S(x_i) > k - 1 \text{ and } i \rightarrow j, \text{ or } G_i^S(x_i) \leq k - 1 \text{ and } i \dashv j \\ \text{undefined} & \text{otherwise} \end{cases} \quad (6)$$

Let $\sigma_{j,i}^S := F_{j,i}^S \circ G_i^S(x_i)$ and where σ_j^S is the vector-valued function with components $\sigma_{j,i}^S$.

In addition, to every node j we assign a rule \bar{M}_j that combines all the values of the input edges to a node j into a single real value x_j . This rule is called a *logic* at the node j and it is assumed to be a multi-affine function with all coefficients equal to 1. Recall that a multi-affine function is a polynomial with the property that the degree in any of its variables is at most 1.

The *S-system* for **RN** is a system of ordinary differential equations

$$\dot{x}_j = -\gamma_j^S x_j + \Lambda_j^S(x) = -\gamma_j^S x_j + \bar{M}_j \circ \sigma_j^S(x) \quad j = 1, \dots, N \quad (7)$$

We will later show the connection between this system and a multi-level discrete function D^S as in (5), and its asynchronous update rule \mathcal{F}^S as in Definition 2.3.

Continuing the example **RN** shown in Figure 1, the corresponding S-system is the system given by

$$\begin{aligned} \dot{x} &= -\gamma_x^S + \sigma_{x,y}^S(y) \\ \dot{y} &= -\gamma_y^S + \sigma_{y,x}^S(x) \end{aligned}$$

where

$$\sigma_{x,y}^S(y) = \begin{cases} u_{x,y}^S & \text{if } y < \theta_{x,y} \\ l_{x,y}^S & \text{if } y > \theta_{x,y}^S \end{cases}; \quad \sigma_{y,x}^S(x) = \begin{cases} u_{y,x}^S & \text{if } x < \theta_{y,x} \\ l_{y,x}^S & \text{if } x > \theta_{y,x} \end{cases}.$$

The function $\sigma_{y,x}^S(x)$ is depicted on the left of Figure 2. The other function $\sigma_{x,y}^S(y)$ will have the same shape, as both edges of the example **RN** correspond to negative regulation.

2.2 L-system

For the L-system we replace a single threshold $\theta_{j,i}$ by two thresholds $\vartheta_{j,i}^-$, and $\vartheta_{j,i}^+$. Given a regulatory network **RN** = (V, E), to each node i we again assign a decay parameter γ_i^L . For each edge $(i, j) \in E$, we associate four real-valued parameters $u_{j,i}^L$, $l_{j,i}^L$, $\vartheta_{j,i}^-$, and $\vartheta_{j,i}^+$. Here again $A_{j,i} := \{l_{j,i}^L, u_{j,i}^L\}$ (Definition 2.2). We require for all i that

$$0 < \gamma_i^L, \quad 0 < l_{j,i}^L < u_{j,i}^L, \quad 0 < \vartheta_{j,i}^- < \vartheta_{j,i}^+, \quad [\vartheta_{j,i}^-, \vartheta_{j,i}^+] \cap [\vartheta_{k,i}^-, \vartheta_{k,i}^+] = \emptyset \text{ whenever } j \neq k.$$

The tuple $z^L = (l^L, u^L, \vartheta^-, \vartheta^+, \gamma^L) \in \mathbb{R}^{d^L}$ is an L-parameter of **RN**, where $d^L = \#(V) + 4\#(E)$.

In an analogy with the S-system, we define a function

$$\sigma_{j,i}^L(x) := \pi_i(\sigma_j^L(x)) = \begin{cases} l_{j,i}^L & \text{for } x_i \leq \vartheta_{j,i}^- \text{ and } i \rightarrow j, \text{ or } x_i \geq \vartheta_{j,i}^+ \text{ and } i \dashv j \\ u_{j,i}^L & \text{for } x_i \geq \vartheta_{j,i}^+ \text{ and } i \rightarrow j, \text{ or } x_i \leq \vartheta_{j,i}^- \text{ and } i \dashv j \\ f_{j,i}^L(x_i) & \text{for } x_i \in [\vartheta_{j,i}^-, \vartheta_{j,i}^+] \end{cases} \quad (8)$$

where $f_{j,i}^L(x_i)$ is a Lipschitz continuous function with lower bound $l_{j,i}^L$ and upper bound $u_{j,i}^L$. The function $\sigma_{j,i}^L(x)$ is a step function that is regularized by a Lipschitz bridge. This defines a vector-valued function $\sigma_j^L(x)$ coordinate-wise.

Definition 2.7. At every L-parameter and for every $i = 1, \dots, N$, the interval $[0, \infty)$ is decomposed into intervals with non-overlapping interiors

$$(I_{0,i} := [0, \vartheta_{j_1,i}^-]) \leq (I_{\frac{1}{2},i} := [\vartheta_{j_1,i}^-, \vartheta_{j_1,i}^+]) \leq (I_{1,i} := [\vartheta_{j_1,i}^+, \vartheta_{j_2,i}^-]) \leq \dots \leq (I_{m_i,i} := [\vartheta_{j_{m_i},i}^-, \infty)).$$

We define the i -th component of the state function G^L (see (1)) by

$$G_i^L(x_i) = k \text{ when } x_i \in \text{int } I_{k,i}.$$

We leave $G_i^L(x_i)$ undefined on finite set of values $x_i = \vartheta_{n,i}^\pm$ where $n = j_1, \dots, j_{m_i}$. Let $\mathcal{V}^L(i) := \{0, \frac{1}{2}, 1, \frac{3}{2}, \dots, m_i\}$ be the range of G_i^L and let $\mathcal{V}^L := \prod_i \mathcal{V}^L(i)$ be the set of states associated to the domains \mathcal{K}^L . Note that G^L induces a bijection g^L between the set of domains \mathcal{K}^L and \mathcal{V}^L , as in (2).

A system of ordinary differential equations is called an *L-system associated to \mathbf{RN}* if

$$\dot{x}_j = -\gamma_j^L x_j + \Lambda_j^L(x) = -\gamma_j^L x_j + \bar{M}_j \circ \sigma_j^L(x) \quad j = 1, \dots, N, \quad (9)$$

where \bar{M}_j is defined as for an S-system.

We continue our example. For network shown in Figure 1, the associated L-system is given by

$$\begin{aligned} \dot{x} &= -\gamma_x^S + \sigma_{x,y}^L(y) \\ \dot{y} &= -\gamma_y^S + \sigma_{y,x}^L(x). \end{aligned}$$

In Figure 2 we depict one possible shape of function $\sigma_{i,j}^L(x_j)$; any continuous function $f_{i,j}^L(x_j)$ that connects $u_{y,x}^L$ and $l_{y,x}^L$ and is bounded vertically between these values satisfies our constraints on $\sigma_{i,j}^L(x_j)$.

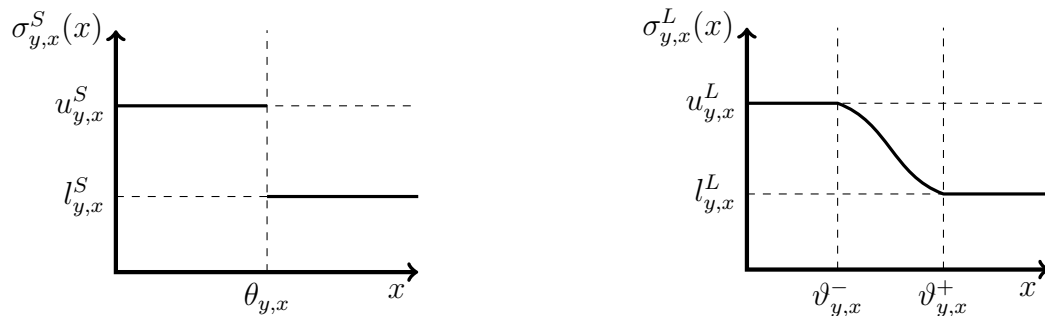


Figure 2: (Left) Function $\sigma_{y,x}^S(x)$ from the S-system associated to \mathbf{RN} shown in Figure 1. (Right) Function $\sigma_{y,x}^L(x)$ from the associated L-system.

It is important to note that the function $\sigma_{j,i}^L(x)$ cannot be represented as a composition $F_{j,i}^L \circ G_i^L$ as in the S-system. This is because the range of $\sigma_{j,i}^L$ is an interval $[l_{j,i}^L, u_{j,i}^L]$, rather than the discrete set of values $\{l_{j,i}^L, u_{j,i}^L\}$. This means that we cannot construct a multi-level discrete function D^L . However, we will construct a nearest neighbor multi-valued function \mathcal{F}^L such that the solutions of L-system are compatible with \mathcal{F}^L .

Systems of ordinary differential equations similar to the L-system have been studied as continuous perturbations of the S-systems [24, 18]. In this interpretation, the interval $[\vartheta_{j,i}^-, \vartheta_{j,i}^+]$ in the definition of $\sigma_{j,i}^L$ contains the threshold $\theta_{j,i}$ of $\sigma_{j,i}^S$, and has length ϵ , a small number. With the same values $l_{j,i}^L = l_{j,i}^S$, and $u_{j,i}^L = u_{j,i}^S$, the function $\sigma_{j,i}^L$ is a small C^0 perturbation of $\sigma_{j,i}^S$. A challenge is to characterize how the dynamics of such a nearby L-system reflect the dynamics of the S-system. This is a difficult question in the ODE setting, where the emphasis is on individual trajectories.

In this paper we address this question from a perspective of global dynamics, where we compare the Morse graphs associated to \mathcal{F}^L and \mathcal{F}^S . Furthermore, we do not require that intervals $[\vartheta_{j,i}^-, \vartheta_{j,i}^+]$ are small; this is replaced by the requirement that $[\vartheta_{j,i}^-, \vartheta_{j,i}^+] \cap [\vartheta_{k,i}^-, \vartheta_{k,i}^+] = \emptyset$.

3 Construction of \mathcal{F}^S and \mathcal{F}^L

In this section we will show that both the S- and L-systems generate nearest neighbor multi-valued functions \mathcal{F}^S and \mathcal{F}^L . We will represent these maps as graphs with vertices that correspond to discrete states, and edges that correspond to allowed transitions.

It is clear from the definition of the S-system that the thresholds $\{\theta_{j,i} : j \in \mathbf{T}(i)\}$ form a strict total order for each $i \in V$. We denote this collection of orderings by $O(z^S)$. Similarly, the intervals $\{[\vartheta_{j,i}^-, \vartheta_{j,i}^+] : j \in \mathbf{T}(i)\}$ form a strict total order for each $i \in V$, and we denote the collection by $O(z^L)$. Note that Λ_j^S and Λ_j^L are multi-affine combinations of bounded functions, so they are themselves bounded.

For convenience we introduce the thresholds $\vartheta_{0,i} = \theta_{0,i} = 0$ and $\vartheta_{\infty,i} = \theta_{\infty,i} = \infty$ for each i .

Definition 3.1. Let φ, φ' be thresholds in either the switching or perturbed systems. We say that φ, φ' are *adjacent* if $\varphi < \varphi'$ and there does not exist φ'' such that $\varphi < \varphi'' < \varphi'$.

Let

$$\zeta := \prod_{i=1}^N I_i$$

where I_i is either a non-degenerate interval $I_i = [\varphi_i, \varphi'_i]$ with adjacent thresholds φ_i, φ'_i , a half-infinite interval $I_i = [\varphi_i, \infty)$ where φ_i is the largest of the thresholds of x_i , or a degenerate interval $I_i = [\varphi_i, \varphi_i]$. Let

$$ND(\zeta) := \{i \in \{1, \dots, N\} \mid I_i \text{ is a non-degenerate interval}\},$$

and let $\ell = \#(ND(\zeta))$. Note that ζ has dimension ℓ in phase space and say that ζ is an ℓ -cell.

If ζ is an N -cell we refer to it as a *domain*. The collection of all domains of S-systems will be denoted by \mathcal{K}^S and the same collection for L-system will be \mathcal{K}^L .

In order to facilitate comparison between domains of S- and L-systems we define two subsets of \mathcal{K}^L . First, we denote $\mathcal{K}_N^L \subsetneq \mathcal{K}^L$ to be the set of domains κ such that for every $i \in ND(\kappa)$, the interval I_i is either half-infinite or of the form $I_i = [\vartheta_{j_m,i}^+, \vartheta_{j_{m+1},i}^-]$. These are the intervals where the functions $\sigma_{j,i}^L(x_i)$ are constant. Second, we define the subset $\mathcal{K}_{N-1}^L \subsetneq \mathcal{K}^L$ such that one and exactly one $\sigma_{j,i}^L(x_i) = f_{ji}^L(x_i)$ is not constant; that is, there is an exactly one $i \in ND(\kappa)$ such that $I_i = [\vartheta_{j,i}^-, \vartheta_{j,i}^+]$ for some j .

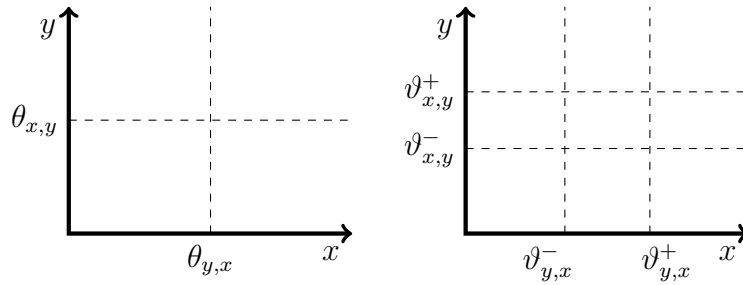


Figure 3: The phase space for the the S-system (left), and L-system (right) associated to RN in Figure 1.

Definition 3.2. Let $\kappa \in \mathcal{K}^S$, or $\kappa \in \mathcal{K}^L$ where $\kappa := \prod_{i=1}^N I_i$ with $I_i = [\varphi_i, \varphi'_i]$, $\varphi_i \neq \varphi'_i$, or half-infinite. Considering I_j , we say that

$$\tau_j^- := \prod_{i=1}^{j-1} I_i \times \{\varphi_j\} \times \prod_{i=j+1}^N I_i$$

is a *left face* of κ with projection index j . Similarly, if $\varphi'_j \neq \infty$, we say that

$$\tau_j^+ := \prod_{i=1}^{j-1} I_i \times \{\varphi'_j\} \times \prod_{i=j+1}^N I_i$$

is a *right face* of κ with projection index j .

A *wall* is a pair (τ, κ) , where κ is a domain and τ is a face of κ . Each wall inherits the projection index from the corresponding face τ of κ . We say the *sign of the wall* (τ, κ) is 1 (and write $\text{sgn}(\tau, \kappa) = 1$) if τ is a left face of κ and we say the sign of the wall (τ, κ) is -1 (and write $\text{sgn}(\tau, \kappa) = -1$) if τ is a right face of κ . We denote the collection of walls by $\mathcal{W}(z)$.

The goal of this section is to define maps \mathcal{F}^S and \mathcal{F}^L on a discrete set of states. The states will be associated to domains \mathcal{K}^S and \mathcal{K}^L . For each pair of domains κ, κ' such that $\tau = \kappa \cap \kappa'$

is a face with some projection index j , we will associate a direction, either $+1$, -1 , or both, to each pair of walls (τ, κ) and (τ, κ') by making use of the sign of these walls. We then finish by associating an oriented edge (or edges) to the pair of states that correspond to κ and κ' .

Observe that by definition of functions $\Lambda(x)$ for either S- or L-system ((7) and (9)), the value of $\Lambda(x)$ is constant on the interior of κ , $\text{int}(\kappa)$, where $\kappa \in \mathcal{K}^S$ for the S-system or $\kappa \in \mathcal{K}_N^L \subsetneq \mathcal{K}^L$ for the L-system. We emphasize that this is not true for domains $\kappa \in \mathcal{K}^L \setminus \mathcal{K}_N^L$ for L-systems, since there is at least one variable $x_i \in [\vartheta_{j,i}^-, \vartheta_{j,i}^+]$.

With a slight abuse of the notation we will call this value $\Lambda(\kappa)$. This value

$$\Lambda(\kappa) = (\Lambda_1(\kappa), \dots, \Lambda_N(\kappa))$$

has a nice interpretation in terms of solutions of the S-system: all solutions starting at $x \in \text{int}(\kappa)$ converge toward the point

$$(\Gamma^S)^{-1}\Lambda^S(\kappa) = (\Lambda_1^S(\kappa)/\gamma_1^S, \dots, \Lambda_N^S(\kappa)/\gamma_N^S),$$

where Γ^S is a diagonal matrix consisting of γ_i^S .

Definition 3.3. The *focal point* or *target point* of a domain $\kappa \in \mathcal{K}^S$ at a valid S-parameter or $\kappa \in \mathcal{K}_N^L$ at a valid L-parameter is the value $\Gamma^{-1}\Lambda(\kappa)$, where $\Gamma = \Gamma^S$, or $\Gamma = \Gamma^L$, respectively. To simplify notation will use notation Γ for both as the superscript will be clear from the context. If $\Gamma^{-1}\Lambda(\kappa) \in \kappa'$ we call κ' a *target domain*. We say that κ is an *attracting domain* if $\Gamma^{-1}\Lambda(\kappa) \in \kappa$.

Definition 3.4. A *regular S-parameter* z^S satisfies for all $i = 1, \dots, N$, $j \in \mathbf{T}(i)$, and $\kappa \in \mathcal{K}^S$,

$$\Lambda_i^S(\kappa)/\gamma_i^S \neq \theta_{j,i}.$$

We call the space of all regular S-parameters Z^S . A *regular L-parameter* z^L satisfies for all $i = 1, \dots, N$, $j \in \mathbf{T}(i)$, and $\kappa \in \mathcal{K}_N^L$,

$$\Lambda_i^L(\kappa)/\gamma_i^L \neq \vartheta_{j,i}^\pm.$$

We call the space of all regular L-parameters Z^L .

3.1 Nearest neighbor multi-valued map \mathcal{F}^S for the S-system

We first define the map D^S which mimics the action of the target point function $\Gamma^{-1}\Lambda : \mathbb{R}^N \rightarrow \mathbb{R}^N$ on the level of states \mathcal{V} . Let $D^S : \mathcal{V}^S \rightarrow \mathcal{V}^S$ by

$$D^S \circ G^S = G^S \circ \Gamma^{-1}\Lambda^S, \tag{10}$$

where recall that G^S is defined in Section 2.1. We now define the map D^S more explicitly. Since $\Gamma^{-1}\Lambda = \Gamma^{-1}\bar{M} \circ \sigma$, let

$$M := \Gamma^{-1}\bar{M}.$$

Then since

$$G^S \circ \Gamma^{-1} \Lambda^S = G^S \circ \Gamma^{-1} \bar{M} \circ \sigma^S = G^S \circ M \circ F^S \circ G^S$$

we have

$$D^S := G^S \circ M \circ F^S,$$

analogously to (5). We now proceed to construct a nearest neighbor multi-valued map \mathcal{F}^S from the focal points of the S-system (7), then we show that \mathcal{F}^S is compatible with the S-system in the sense of Definition 2.6, and, finally, we show that \mathcal{F}^S is an asynchronous update rule for D^S .

Definition 3.5. Let z^S be a regular parameter for an S-system and \mathcal{K}^S the corresponding set of domains. The *wall-labeling* of $\mathcal{W}(z^S)$ is a function $\mathcal{L}^S : \mathcal{W}(z^S) \rightarrow \{-1, 1\}$ defined as follows. Let $(\tau, \kappa) \in \mathcal{W}(z^S)$ be a wall with projection index j ; i.e. $\tau \subset \{x_i = \theta_{j,i}\}$. Then define

$$\mathcal{L}^S((\tau, \kappa)) := \text{sgn}(\tau, \kappa) \cdot \text{sgn}(\Lambda_i^S(\kappa)/\gamma_i^S - \theta_{j,i}).$$

A wall (τ, κ) is an *absorbing wall* if $\mathcal{L}^S((\tau, \kappa)) = -1$ and an *entrance wall* if $\mathcal{L}^S((\tau, \kappa)) = 1$.

Notice that a regular parameter enforces $\Lambda_i(\kappa)/\gamma_i - \theta_{ji} \neq 0$, so that $\mathcal{L}^S((\tau, \kappa))$ is defined for all walls.

Definition 3.6. Let z^S be a regular parameter for an S-system, with \mathcal{K}^S the corresponding set of domains, \mathcal{V}^S the set of states, and the state function G^S , which induces the bijection $g^S : \mathcal{K}^S \rightarrow \mathcal{V}^S$ described in Definition 2.2.

We define a multi-valued function $\mathcal{F}^S : \mathcal{V}^S \rightrightarrows \mathcal{V}^S$ induced by the wall-labeling \mathcal{L}^S as follows. Let $g^S(\kappa_1) = s_1$ and $g^S(\kappa_2) = s_2$. Then $s_2 \in \mathcal{F}^S(s_1)$ if and only if one of the following holds:

- (a) $s_1 = s_2$ and κ is an attracting domain.
- (b) There exists some face τ such that (τ, κ_1) and (τ, κ_2) are walls and $\mathcal{L}^S((\tau, \kappa_1)) = -1$ (indicating an absorbing wall of κ_1) and $\mathcal{L}^S((\tau, \kappa_2)) = 1$ (indicating an entrance wall of κ_2).

As in Definition 2.3 we may represent \mathcal{F} as a graph $(\mathcal{V}^S, \mathcal{E}^S)$, where $(s_1, s_2) \in \mathcal{E}^S$ if and only if $s_2 \in \mathcal{F}^S(s_1)$. We call this graph a *state transition graph* of the S-system.

Theorem 3.7. \mathcal{F}^S is compatible with the S-system.

Proof. The key observation is that all solutions in $\text{int}(\kappa)$ converge toward the target point $\Gamma^{-1}\Lambda(\kappa)$, while they lie within κ . If there is no trajectory leaving κ for an adjacent domain, then the trajectory x must remain within κ for all time. Hence the focal point $\Gamma^{-1}\Lambda(\kappa)$ is in κ , and κ is an attracting domain. By Definition 3.6 (a), $s \in \mathcal{F}^S(s)$, where $s = g^S(\kappa)$.

Now assume that there exists a trajectory $x(t) = (x_1(t), \dots, x_N(t))$ that passes from κ_1 to an adjacent κ_2 via an intervening face τ , where $x_i = \theta_{j,i}$ on τ . First consider the case in which τ is a right face of κ_1 and a left face of κ_2 , so that $\text{sgn}(\tau, \kappa_1) = -1$ and $\text{sgn}(\tau, \kappa_2) = 1$. Let $x_i(0) = \theta_{j,i}$. There is an interval $I := (-\epsilon, \epsilon) \subset \mathbb{R}$ such that $\dot{x}_i(t) > 0$ for all $t \in I \setminus \{0\}$

and $x(t) \in \kappa_1$ for $t \in (-\epsilon, 0)$, $x(t) \in \kappa_2$ for $t \in (0, \epsilon)$. Let $t_k = \Lambda_i^S(\kappa_k)/\gamma_i^S$ for $k = 1, 2$ denote the target points of the domains. Then $\dot{x}_i(t) > 0$ implies $t_1, t_2 > \theta_{j,i}$, which implies

$$\mathcal{L}^S((\tau, \kappa_1)) = -1 \cdot 1 \text{ and } \mathcal{L}^S((\tau, \kappa_2)) = 1 \cdot 1.$$

Thus $s_2 \in \mathcal{F}^S(s_1)$, where $s_k := g^S(\kappa_k)$, by Definition 3.6 (b).

The case in which $\text{sgn}(\tau, \kappa_1) = 1$ and $\text{sgn}(\tau, \kappa_2) = -1$ with $\dot{x}_i(t) < 0$ on I is similar. \square

The proof of the following theorem we postpone to Appendix A due to length.

Theorem 3.8. \mathcal{F}^S is an asynchronous update rule for D^S .

3.2 Nearest neighbor multi-valued map \mathcal{F}^L for the L-system

Definition 3.3 defines focal points for all domains $\kappa \in \mathcal{K}^S$, but only for domains $\kappa \in \mathcal{K}_N^L \subsetneq \mathcal{K}^L$ in the L-system. Therefore, we cannot construct a multi-level map D^L analogous to D^S for the S-system, and moreover the wall labeling that we used to construct \mathcal{F}^S cannot be used in the same way for $\kappa \in \mathcal{K}^L$ to define \mathcal{F}^L . But it turns out that all the information needed to assign directions to all walls in the L-system can be inferred from just the domains in \mathcal{K}_N^L . We will use this fact to construct an nearest neighbor multi-valued map \mathcal{F}^L and associated state transition graph $(\mathcal{V}^L, \mathcal{E}^L)$, without going through the map D^L as an intermediary.

Definition 3.9. Recall from Definition 3.1 that an ℓ -cell has the form $\zeta = \prod_{i=1}^N [\varphi_i, \varphi'_i]$. We define the set of *corner points* of ζ , denoted $\mathcal{C}(\zeta)$, by

$$\mathcal{C}(\zeta) := \prod_{i=1, \varphi'_i \neq \infty}^N \{\varphi_i, \varphi'_i\},$$

Note that we exclude $\varphi'_i = \infty$ from the definition of corner points.

Definition 3.10. Let $\mathcal{C}(\zeta)$ be the set of corner points for an ℓ -cell ζ for an L-system with regular parameter z^L , and let $P, P' \in \mathcal{C}(\zeta)$ be corner points with $P = (\varphi_1, \varphi_2, \dots, \varphi_N)$ and $P' = (\varphi'_1, \varphi'_2, \dots, \varphi'_N)$. We introduce the function $\text{Sign}(\mathcal{C}(\zeta), k)$ defined as

$$\text{Sign}(\mathcal{C}(\zeta), k) = \begin{cases} +1 & \text{if } \forall P \in \mathcal{C}(\zeta), \Lambda_k(P)/\gamma_k - \varphi_k > 0 \\ -1 & \text{if } \forall P \in \mathcal{C}(\zeta), \Lambda_k(P)/\gamma_k - \varphi_k < 0 \\ 0 & \text{if } \exists P, P' \in \mathcal{C}(\zeta) \text{ such that } \Lambda_k(P)/\gamma_k - \varphi_k > 0 \text{ and } \Lambda_k(P')/\gamma_k - \varphi'_k < 0 \end{cases} \quad (11)$$

Notice that a regular parameter enforces $\Lambda_k^L(P)/\gamma_k - \varphi_k \neq 0$, so that (11) covers all possible cases. Note also that since the intervals $[\vartheta_{k,i}^-, \vartheta_{k,i}^+]$ are disjoint for all k , the i -th component of every corner point of ζ is on the boundary of the set $\mathbb{R} \setminus \bigcup_k [\vartheta_{k,i}^-, \vartheta_{k,i}^+]$. Therefore every corner point of ζ is also the corner point of some $\kappa \in \mathcal{K}_N^L$.

Definition 3.11. Let $z^L \in Z^L$ be a regular parameter. The *wall-labeling* of $\mathcal{W}(z^L)$ is a function $\mathcal{L}^L : \mathcal{W}(z^L) \rightarrow \{-1, 0, 1\}$ defined as follows. Let $(\tau, \kappa) \in \mathcal{W}(z^L)$ have a projection index i . Then define

$$\mathcal{L}^L((\tau, \kappa)) := \text{sgn}(\tau, \kappa) \cdot \text{Sign}(\mathcal{C}(\tau), i)$$

A wall (τ, κ) is an *absorbing wall* if $\mathcal{L}^L((\tau, \kappa)) = -1$, an *entrance wall* if $\mathcal{L}^L((\tau, \kappa)) = 1$, and a *bidirectional wall* if $\mathcal{L}^L((\tau, \kappa)) = 0$.

Definition 3.12. Let z^L be a regular parameter for an L-system, \mathcal{K}^L be the corresponding set of domains, \mathcal{V}^L be the state space and $g^L : \mathcal{K}^L \rightarrow \mathcal{V}^L$ be the bijection between the set of domains \mathcal{K}^L and the states \mathcal{V}^L .

The nearest neighbor multi-valued map $\mathcal{F}^L : \mathcal{V}^L \rightrightarrows \mathcal{V}^L$ induced by the wall-labeling \mathcal{L}^L is defined as follows. Let $g^L(\kappa_1) = s_1$ and $g^L(\kappa_2) = s_2$. Then $s_2 \in \mathcal{F}^L(s_1)$ if and only if one of the following holds:

- a) $s_1 = s_2$ and $\kappa \in \mathcal{K}_N^L$ is an attracting N -domain.
- b) There exists some face τ such that (τ, κ_1) and (τ, κ_2) are walls and $\mathcal{L}^L((\tau, \kappa_1)) = -1$ (indicating an absorbing wall of κ_1) and $\mathcal{L}^L((\tau, \kappa_2)) = 1$ (indicating an entrance wall of κ_2).
- c) There exists some face τ such that (τ, κ_1) and (τ, κ_2) are walls and $\mathcal{L}^L((\tau, \kappa_1)) = \mathcal{L}^L((\tau, \kappa_2)) = 0$ (indicating a bidirectional wall of both κ_1 and κ_2).

Remark 3.13. We want to make two notes about this definition.

- First, since attracting domains are only defined for $\kappa \in \mathcal{K}_N^L \subsetneq \mathcal{K}^L$ we can only have self-edges on N -domains. We justify this choice later by showing that there is always an escape path out of any $\kappa \in \mathcal{K}^L \setminus \mathcal{K}_N^L$, see Lemma C.4.
- Second, notice that if there exist two domains κ_1, κ_2 in an L-system phase space sharing a face τ , then $\mathcal{L}^L((\tau, \kappa_1)) = 0$ if and only if $\text{Sign}(\mathcal{C}(\tau), i) = 0$, which happens if and only if $\mathcal{L}^L((\tau, \kappa_2)) = 0$. Therefore there is never a case where $\mathcal{L}^L((\tau, \kappa_1)) = \pm 1$ and $\mathcal{L}^L((\tau, \kappa_2)) = 0$, which shows that the assignment of arrows is always well defined.

Theorem 3.14. *The L-system is compatible with the nearest neighbor multivalued map \mathcal{F}^L .*

Proof. If there is no trajectory leaving $\kappa \in \mathcal{K}_N^L$ for an adjacent domain, then the trajectory x must remain within κ for all time. Hence the focal point $\Gamma^{-1}\Lambda^L(\kappa)$ is in κ , and κ is an attracting domain. By Definition 3.12 (a), $s \in \mathcal{F}^S(s)$, where $s = g^S(\kappa)$.

Now assume that there exists a trajectory that passes from κ_1 to an adjacent κ_2 via an intervening face τ . First consider the case in which τ is a right face of κ_1 and a left face of κ_2 , so that $\text{sgn}(\tau, \kappa_1) = -1$ and $\text{sgn}(\tau, \kappa_2) = 1$. Then $\dot{x}_i > 0$ on τ and thus

$$\text{Sign}(\mathcal{C}(\tau), i) \in \{0, +1\}$$

since $\text{Sign}(\mathcal{C}(\tau), i) = -1$ implies $\dot{x}_i < 0$ everywhere on τ by Theorem B.2. If $\text{Sign}(\mathcal{C}(\tau), i) = +1$, then

$$\mathcal{L}^L((\tau, \kappa_1)) = -1 \cdot 1; \quad \mathcal{L}^L((\tau, \kappa_2)) = 1 \cdot 1,$$

and $s_2 \in \mathcal{F}^S(s_1)$, where $s_k := g^S(\kappa_k)$, by Definition 3.12 (b). Likewise if $\text{Sign}(\mathcal{C}(\tau), i) = 0$, then

$$\mathcal{L}^L((\tau, \kappa_1)) = \mathcal{L}^L((\tau, \kappa_1)) = 0,$$

and $s_2 \in \mathcal{F}^S(s_1)$ by Definition 3.12 (c).

The case when $\text{sgn}(\tau, \kappa_1) = 1$ and $\text{sgn}(\tau, \kappa_2) = -1$ is similar. \square

4 Relating \mathcal{F}^S and \mathcal{F}^L

We want to compare dynamics of the multi-valued maps \mathcal{F}^S and \mathcal{F}^L that are associated to the same network $\mathbf{RN} = (V, E)$. Dynamics in our interpretation is characterized by the Morse graph and so our questions will be about the relationship between Morse graphs. Multi-valued maps are also parameterized by parameters $z^S \in Z^S, z^L \in Z^L$ and therefore this comparison must be performed between related parameters. Our goal is to define a canonical map between from the set of regular parameters Z^S to the set of regular parameters Z^L .

We make the following key observations

- For both S- and L-systems, the order of the thresholds determines an order of activation (or deactivation) of the targets of node i as x_i increases;
- the images of the maps \mathcal{F}^S and \mathcal{F}^L depend only on the target *domains*, rather than target points in these domains. Based on these facts, we define an equivalence relation on the set of regular parameters $z^S, v^S \in Z^S$ and an analogous equivalence relationship on the set of regular parameters $z^L, v^L \in Z^L$.

Definition 4.1. Let \mathbf{RN} be a regulatory network. Let $O = \{O_i\}$ be a collection of orders of the target nodes of node i :

$$O_i = \{j_1 < j_2 < \dots < j_{m_i} \mid j_k \in \mathbf{T}(i)\}.$$

Let z be a regular parameter of either an S- or L-system. We say that O is the *threshold order* of z , and denote it $O(z)$, if $\theta_{j_k, i} < \theta_{j_l, i}$ in z^S or $[\vartheta_{j_k, i}^-, \vartheta_{j_k, i}^+] < [\vartheta_{j_l, i}^-, \vartheta_{j_l, i}^+]$ in z^L if and only if $j_k < j_l$ in O_i .

Recall that $\mathcal{V}^S(i) = \{0, 1, 2, \dots, m_i\}$ and $\mathcal{V}^L(i) = \{0, \frac{1}{2}, 1, \frac{3}{2}, 2, \dots, m_i\}$. Note that

$$\Psi : \mathcal{V}^S \leftrightarrow \mathcal{V}^L \text{ by } \Psi(v) = v,$$

which is a bijection onto its image

$$\mathcal{V}^{SL} := \Psi(\mathcal{V}^S).$$

Since $\mathcal{V}^{SL} = g^L(\mathcal{K}_N^L)$ is a bijection and by the definition of the L-system the target points are defined for $\kappa \in \mathcal{K}_N^L$, we define a multi-level discrete map D_N^L for the L-system by

$$D_N^L : \mathcal{V}^{SL} \rightarrow \mathcal{V}^L \text{ by } D_N^L := (g^L)^{-1} \circ \Gamma^{-1} \Lambda^L(\kappa) \circ g^L$$

which captures the location of the focal point for each $\kappa \in \mathcal{K}_N^L$. Note that this multi-level map D_N^L over the subset \mathcal{V}^{SL} does not uniquely determine a map D^L over \mathcal{V}^L .

Definition 4.2. We say that two regular parameters $z^S, v^S \in \mathcal{Z}^S$ are equivalent,

$$z^S \stackrel{S}{\sim} v^S$$

if the following hold:

- (1) $O(z^S) = O(v^S)$ and
- (2) $D^S(z^S) = D^S(v^S)$, where $D^S(z^S)$ and $D^S(v^S)$ are the multi-level discrete maps induced by z^S and v^S respectively.

We denote the equivalence classes of $\stackrel{S}{\sim}$ by \mathcal{Z}^S , and say $\omega^S \in \mathcal{Z}^S$. We shall use the notation $O(\omega^S)$ to denote the constant threshold order for all $z^S \in \omega^S$, and use $D^S(\omega^S)$ to denote the fixed multi-level discrete map valid for all parameters in this equivalence class.

The equivalence relationship $\stackrel{L}{\sim}$ between $z^L, v^L \in \mathcal{Z}^L$ is defined analogously using the map D_N^L . Notation $\omega^L \in \mathcal{Z}^L$, $O(\omega^L)$, and $D_N^L(\omega^L)$ is also analogous.

Remark 4.3. Note that the maps \mathcal{F}^S and \mathcal{F}^L only depend on the equivalence class ω^S and ω^L , respectively, and not on individual parameters $z^S \in \omega^S$, or $z^L \in \omega^L$. This is because the wall-labeling functions \mathcal{L}^S and \mathcal{L}^L depend only the location of target points $\Gamma^{-1}\Lambda(\kappa)$ with respect to thresholds. Therefore the Morse graph **MG**, which we view as a summary of dynamics of \mathcal{F} , is also only a function of the equivalence class ω . With a slight abuse of notation we will denote by $\mathcal{F}^S(\omega^S)$ the map \mathcal{F}^S that corresponds to any parameter $z^S \in \omega^S$. Similar notation will be used for the map \mathcal{F}^L .

As an aside, note that the elements of \mathcal{Z}^S correspond to the nodes of a *combinatorial parameter graph*, introduced in [12]. The edges in this graph correspond to a single change in the order of indices in O_i for a single i , or to a change in the i -th component from one target state to an adjacent target state for a single i .

Definition 4.4. The *canonical map* $\Omega : \mathcal{Z}^S \hookrightarrow \mathcal{Z}^L$ maps $\omega^S \in \mathcal{Z}^S$ to $\omega^L \in \mathcal{Z}^L$ if and only if

1. $O(\omega^S) = O(\omega^L)$ and
2. $D^S(\omega^S) = D_N^L(\omega^L)$.

It is easy to see that for a fixed network **RN** the map Ω is injective.

At this point we are ready to precisely formulate a central question of this paper. For a fixed network **RN** we have introduced two different classes of multi-valued maps $\mathcal{F}^S(\omega^S)$ and $\mathcal{F}^L(\omega^L)$ motivated by S- and L-systems of differential equations. These are both valid choices of a model that captures the dynamics of the network, and they both describe a family of dynamical models that depend in a continuous way on a high dimensional set of parameters. In Remark 4.3 we have shown that the number of dynamical behaviors, as captured by the Morse graphs, is finite, as it only depend on the equivalence class $\omega \in \mathcal{Z}$, and \mathcal{Z} is a finite set. Finally, in (4.4) we have shown that there is a bijection Ω between \mathcal{Z}^S

and a subset of \mathcal{Z}^L . A natural question is, what is the relationship between the dynamics of $\mathcal{F}^S(\omega)$ and $\mathcal{F}^L(\Omega(\omega))$? More precisely, what is the correspondence between the Morse graphs of $\mathcal{F}^S(\omega)$ and $\mathcal{F}^L(\Omega(\omega))$? The rest of the paper is devoted to this question.

5 Morse graphs of $\mathcal{F}^S(\omega)$ and $\mathcal{F}^L(\Omega(\omega))$

The results in this section depend on the absence of negative self-regulation, which we assumed in the definition of a regulatory network at the beginning of this work. In the Appendix, we prove two important, but technical, lemmas that are the basis of the theorems in this section.

- Lemma C.2 states that an edge $v \rightarrow v'$ in the state transition graph of the S-system exists if and only if the path $\Psi(v) \rightarrow u \rightarrow \Psi(v')$ exists in the L-system state transition graph, where $u = g^L(\eta)$ with $\eta \in \mathcal{K}_{N-1}^L$ is uniquely defined. This implies that every path that exists in \mathcal{V}^S can be lifted to a path in \mathcal{V}^L by adding intermediate nodes u that correspond to domains $\eta := (g^L)^{-1}(u)$ that belong to \mathcal{K}_{N-1}^L . This leads immediately to Corollary C.3, which extends the result to a path of any length in the graph $(\mathcal{V}^S, \mathcal{E}^S)$ generated by \mathcal{F}^S . In other words, paths in $(\mathcal{V}^S, \mathcal{E}^S)$ are equivalent to a select set of paths in $(\mathcal{V}^L, \mathcal{E}^L)$.
- Lemma C.4 proves that if $w \in \mathcal{V}^L$ has $n > 0$ non-integer values, then there exists $w' \in \mathcal{V}^L$ such that $(w, w') \in \mathcal{E}^L$ and w' has $n - 1$ non-integer values. Therefore for any state $w \in \mathcal{V}^L$, there is a path from w to w'' with $(g^L)^{-1}(w'') \in \mathcal{K}_N^L$. In other words, every node in \mathcal{V}^L has a path to a node in \mathcal{V}^{SL} . This is our justification for defining self-edges in the L-system state transition graph based only on states corresponding to $\kappa \in \mathcal{K}_N^L$.

We now proceed to the main theorems of the section that describe the characteristics of a map between the Morse graphs of $\mathcal{F}^S(\omega)$ and $\mathcal{F}^L(\Omega(\omega))$.

Definition 5.1. A map $f : X \rightarrow Y$ between ordered spaces (X, \leq) and (Y, \leq) is *order preserving* if $x_1 < x_2$ implies $f(x_1) \leq f(x_2)$.

Definition 5.2. Referring back to Definition 2.5, let $U, V \in \text{MD}$ be two sets in a Morse decomposition. We define the order $U \preceq V$ only if there exists a path from an element $v \in V$ to an element $u \in U$ in the associated state transition graph of \mathcal{F} . The inequality is strict if there is no return path.

Theorem 5.3. Consider $\omega^S \in \mathcal{Z}^S$ and the nearest neighbor multi-valued maps $\mathcal{F}^S(\omega^S)$ and $\mathcal{F}^L(\Omega(\omega^S))$. Consider the associated Morse graphs MD^S and MD^L . Then there is order-preserving map

$$\phi : \text{MD}^S \rightarrow \text{MD}^L,$$

defined by $C' := \phi(C)$ where C' is the smallest (under inclusion) element of MD^L containing the states $\Psi(C) := \{\Psi(v) \mid v \in C\}$.

Proof. Since $U, V \in \text{MD}^S$, they are strongly connected components of the graph induced by \mathcal{F}^S , there a path between any pair of nodes in U and any pair of nodes in V . By Corollary C.3 the paths between the nodes in U and the nodes of V lift to paths in the graph of \mathcal{F}^L . Therefore the sets $\Psi(U)$ and $\Psi(V)$ are also strongly connected. Therefore $\Psi(U)$ and $\Psi(V)$ must be subsets of Morse sets in MD^L , say $U', V' \in \text{MD}^L$, respectively. We define $U' := \phi(U)$ and $V' := \phi(V)$.

Finally, if $U \preceq V$ in MD^S , there must be a path from an element $v \in V$ to an element $u \in U$. By Corollary C.3 there is a path from $\Psi(v)$ to $\Psi(u)$ in the graph of \mathcal{F}^L and therefore $U' \preceq V'$ in MD^L . This finishes the proof. \square

Notice that in the proof of Theorem 5.3, we cannot conclude that if $U \prec V$ then $U' \prec V'$, only that $U' \preceq V'$. As we will see later, it may be that $U \prec V$ but $V' = U'$. Theorem 5.3 shows that the general ordering of Morse sets remains similar between the two systems. However, the property of order preservation is not very strong and we will examine ways that we can strengthen this result, as well as reasons why this fails in general case.

Definition 5.4. An attractor in a Morse graph MG is a minimal element in the partial order, represented by its Morse set $A \in \text{MD}$. The collection of all attractors of MD^* of the map $\mathcal{F}^*(\omega)$ at $\omega \in \mathcal{Z}^*$ will be denoted by \mathcal{A}^* for both $* = S, L$. We will call all Morse sets that are not attractors *unstable Morse sets*.

Note that the minimality of the attractor in the partial order implies that

- Every forward path starting in an attractor remains in the attractor.
- Every state has a forward path to an attractor.

Theorem 5.5. Consider a network \mathbf{RN} with associated multi-valued maps $\mathcal{F}^S(\omega^S)$ and $\mathcal{F}^L(\Omega(\omega^S))$, and associated Morse decompositions MD^S and MD^L . Then the order preserving map $\phi : \text{MD}^S \rightarrow \text{MD}^L$ restricts to a surjection over the sets of attractors

$$\phi : \mathcal{A}^S \xrightarrow{\text{onto}} \mathcal{A}^L.$$

Proof. Let $A^S \in \mathcal{A}^S \subset \mathcal{V}^S$ be an attractor in MD^S . Since A^S is a strongly connected subgraph, for any $v, v' \in A^S$ there exists a path $v \rightarrow \dots \rightarrow v'$ in the state transition graph of \mathcal{F}^S . Let $w := \Psi(v)$ and $w' := \Psi(v')$. By Corollary C.3, there is then a path from w to w' in the state transition graph of \mathcal{F}^L . Let

$$U := \{w' \in \mathcal{V}^L \mid \text{there is a path from any } w \in \Psi(A^S) \text{ to } w' \in \mathcal{V}^L\}.$$

and let A be the maximal strongly connected subgraph containing U . Clearly, A is an attractor in \mathcal{A}^L . It follows from the definition of ϕ that

$$\phi(A^S) = A.$$

We now need to show that the restriction of ϕ on \mathcal{A}^S is a surjection.

Consider an arbitrary attractor $A^L \subset \mathcal{A}^L$. If $u \in A^L$ such that $(g^L)^{-1}(u) \notin \mathcal{K}_N^L$, by Lemma C.4 there is a path from u to u' with $u' = g^L(\kappa)$ for some $\kappa \in \mathcal{K}_N^L$. Since forward paths starting at $u \in A^L$ remain in A^L by definition of the attractor, we conclude that A^L must contain the vertex u' . To prove ϕ is surjective, we assume by contradiction that there is $A^L \subset \mathcal{A}^L$ such that $A^L \neq \phi(A^S)$ for any attractor $A^S \in \mathcal{A}^S$. By the argument above, there is a vertex $u' \in A^L$ such that $u' = g^L(\kappa)$ for some $\kappa \in \mathcal{K}_N^L$. Let $\Psi^{-1}(u') =: v' \in \mathcal{V}^S$. There must be an attractor A_1^S and $v \in A_1^S$ such that there is a path from v' to v in the state transition graph of \mathcal{F}^S . By Corollary C.3 this path can be lifted to a path from u' to $w := \Psi(v)$ in the state transition graph of \mathcal{F}^L . Since $u' \in A^L$ it must be that $w \in A^L$ and by construction of the map ϕ , $w \in A_1^L := \phi(A_1^S)$. However, since any attractor must contain all of its forward paths and $u' \in A^L$, this implies that $A^L \supseteq A_1^L$. Since A_1^L is maximal by construction, $A^L = A_1^L = \phi(A_1^S)$. This contradicts the assumption that $A^L \neq \phi(A^S)$, which proves the theorem. \square

Theorem 5.5 says the the long term behavior of \mathcal{F}^S captures all long time behavior of the richer map \mathcal{F}^L at the corresponding parameters for networks with no negative self-regulation. Attractors of \mathcal{F}^S can disappear under this correspondence Ω but they cannot be created when employing the class of models \mathcal{F}^L . The assumption that **RN** does not contain a negative self-loop is essential here. In fact that result is not true when there is negative self-regulation [24], because then fixed points may appear in domains $\kappa \in \mathcal{K}^L \setminus \mathcal{K}_N^L$.

We show a stronger relationship between the specific types of attractors of \mathcal{F}^S and \mathcal{F}^L .

Definition 5.6. Let \mathcal{A}^* be the set of attractors associated to a map $\mathcal{F}^*(\omega)$, where $\omega \in \mathcal{Z}^*$ and $*$ = S, L . Define $\text{FP}^* \subset \mathcal{A}^*$ to be the set of attractors that consist of a single vertex $v \in \mathcal{V}^*$. We call $A \in \text{FP}^*$ a *fixed point*.

Theorem 5.7. Consider a network **RN** with associated multi-valued maps $\mathcal{F}^S(\omega^S)$ and $\mathcal{F}^L(\Omega(\omega^S))$. Let FP^S and FP^L be the associated sets of fixed points. Then the restriction of ϕ to FP^S is a bijection

$$\phi : \text{FP}^S \rightarrow \text{FP}^L.$$

Proof. Consider $w \in \text{FP}^L$. Then by Lemma C.4 the domain $\kappa := (g^L)^{-1}(w)$ must be an N-domain $\kappa \in \mathcal{K}_N^L$, and therefore $v := \Psi^{-1}(w) \in \mathcal{V}^S$. Then it follows from Corollary C.3 that since there are no paths that exit w in \mathcal{V}^L , there are no exiting paths from v in \mathcal{V}^S . Therefore $v \in \text{FP}^S$. \square

We now present important examples that show that these results cannot be strengthened in several natural directions. Assume in all statements below that $\eta = \Omega(\omega)$. We will show that

1. The map $\phi : \text{MD}^S(\omega) \rightarrow \text{MD}^L(\eta)$ does not have to be surjective, see Lemma 6.1.
2. The map $\phi : \text{MD}^S(\omega) \rightarrow \text{MD}^L(\eta)$ does not have to be injective, see Lemma 6.4.
3. The map $\phi : \mathcal{A}^S(\omega) \rightarrow \mathcal{A}^L(\eta)$ does not have to be injective, see Lemma 6.5.

6 Examples

We will now present a series of examples illustrating differences which can arise between \mathcal{F}^S and \mathcal{F}^L . In all of the following examples, for clarity we suppose that parameterS $\gamma_i^S = \gamma_i^L = 1$ for all $i \in \{1, \dots, N\}$.

We will be comparing the Morse graph of the S-system to the Morse graph of the L-system under the canonical parameter map Ω . Each equivalence class $\omega \in \mathcal{Z}^S$, or $\Omega(\omega) \in \mathcal{Z}^L$ is represented by a collection of inequalities. The inequalities determine the order of the thresholds and the images of maps D^S and D_N^L for every state simultaneously. For example, suppose we have the nodes $i, j, k, m, n \in \mathbf{RN}$, with i, j additive, positive inputs to node k , and m, n the outputs of k . Assume that i and j only affect node k , so that they each have two states, 0 and 1. Since k has two output thresholds, it has three states, 0, 1, and 2. Suppose further that we have the inequality description

$$l_{k,i} + l_{k,j} < \theta_{m,k} < u_{k,i} + l_{k,j} < \theta_{n,k} < l_{k,i} + u_{k,j} < u_{k,i} + u_{k,j} \quad (12)$$

for the node k . This implies that the threshold order of k is

$$O_k = \{m < n\}$$

and that the k -th component of the map D^S is

$$00 \mapsto 0, \quad 10 \mapsto 1, \quad 01 \mapsto 2, \quad 11 \mapsto 2$$

This happens because when i, j are in their 0 states, they are contributing a low value l , and when they are in their higher 1 states, they are contributing a high value u to node k . A complete description of $\omega \in \mathcal{Z}^S$ includes inequality description like (12) for every node $k \in \mathbf{RN}$.

In this section all the explicit examples of differential equations will be those of S-systems. We therefore drop the superscript S on functions σ^S , and will use σ^- and σ^+ to denote piecewise constant nonlinearities that correspond to negative versus positive regulation in \mathbf{RN} , respectively. See Figure 2 (left) for an example of σ^- . In σ^+ , the lower constant value would occur first.

Lemma 6.1. *The map $\phi : \mathbf{MD}^S \rightarrow \mathbf{MD}^L$ is, in general, not surjective.*

Proof. Consider the network shown in Figure 1, with system of equations

$$\dot{x} = -\gamma_x x + \sigma_{x,y}^-(y), \quad \dot{y} = -\gamma_y y + \sigma_{y,x}^-(x) \quad (13)$$

and $\omega \in \mathcal{Z}^S$ satisfying

$$l_{x,y} < \theta_{y,x} < u_{x,y}, \quad l_{y,x} < \theta_{x,y} < u_{y,x}. \quad (14)$$

The corresponding graphs of $\mathcal{F}^S(\omega)$ and $\mathcal{F}^L(\Omega(\omega))$ are shown in Figure 4, along with the corresponding Morse graphs. It is clear that there cannot exist a surjective map from \mathbf{MD}^S to \mathbf{MD}^L , since \mathbf{MD}^L has an extra unstable Morse set. \square

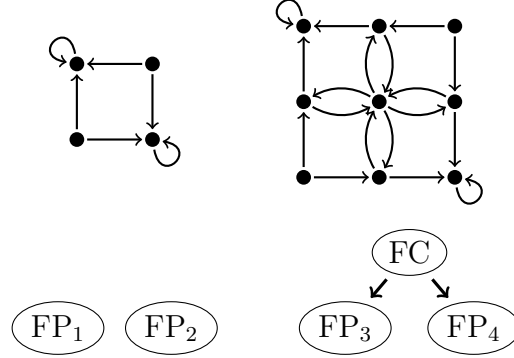


Figure 4: The corresponding $\mathcal{F}^S(\omega)$ (top left) and $\mathcal{F}^L(\Omega(\omega))$ (top right) domain graphs of the bistable example network under a canonical map. Also shown are the Morse graphs of $\mathcal{F}^S(\omega)$ (bottom left) and $\mathcal{F}^L(\Omega(\omega))$ (bottom right).

In Figure 4, the nodes in the Morse graphs labeled FP are fixed points in the set FP. These correspond in both state transition graph (STG) to states with the self loops. The Morse set labeled FC is an unstable Morse set composed of all of the nodes that are not in the corners of STG. Thus Morse set FC is generated by the strongly connected four-leaf clover structure in the middle of the STG, and is clearly unstable since it has paths to the fixed points. Since it is composed of more than one node this Morse set is consistent with cyclic behavior in STG. Since there is cyclic behavior for all (both) variables of the system, we will call this type of Morse set a “full cycle”, or FC. When there is a Morse set with cyclic behavior in a subset of all variables, we will label it XC.

Though Lemma C.2 does guarantee that each path in the graph of \mathcal{F}^S has a corresponding path in the graph of \mathcal{F}^L , the converse is not necessarily true. This insight is key to understanding the limits on the relationship induced by the map ϕ . To illustrate this fact, we will construct the following examples in multiple steps. We first start from simple two dimensional networks and the successively embed this example to more and more complicated examples all the way to five-dimensional networks. The lower dimensional examples establish how paths can exist in the graph of \mathcal{F}^L that have no correlate in \mathcal{F}^S .

First consider the (partial) network $z \dashv y$ with $l_{y,z} < \theta_{*,y} < u_{y,z}$ where $\theta_{*,y}$ is an unspecified threshold of y , and suppose that $\dot{z} < 0$. Notice that this is only part of a network in the sense that we would need at least one other interaction in order to define the threshold of y . This will be resolved when we embed this interaction into a three-dimensional network. The S-system state transition graph is shown in Figure 5 on the left, and the one for the L-system on the right, where recall $\Psi : \mathcal{V}^S \rightarrow \mathcal{V}^{SL}$ is the map between states in the S- and L-systems. Notice that paths between v_i and v_j that exist in the S-system graph map to paths between $\tilde{v}_i := \Psi(v_i)$ and $\tilde{v}_j := \Psi(v_j)$ with intermediate nodes corresponding to (N-1)-domains (see Lemma C.2). However, there is now a path from \tilde{v}_3 to \tilde{v}_2 which does not contain \tilde{v}_1 , shown in cyan. The structure of the graph shown in Figure 5 on the right will play a key role in all later examples. We will embed this structure into higher dimensional state transition graphs.



Figure 5: The fundamental structures of $\mathcal{F}^S(\omega)$, shown left, and $\mathcal{F}^L(\Omega(\omega))$, shown right, where $\tilde{v}_i := \Psi(v_i)$. Note the path from \tilde{v}_3 to \tilde{v}_2 , shown in cyan, does not contain \tilde{v}_1 . This structure will be embedded in all later examples.

Lemma 6.2. *Consider the graphs for $\mathcal{F}^S(\omega)$ and $\mathcal{F}^L(\Omega(\omega))$. A path from $\Psi(v_i)$ to $\Psi(v_j)$ in the graph of \mathcal{F}^L does not guarantee the existence of a path from v_i to v_j in the graph of \mathcal{F}^S .*

Proof. We will now embed the previous partial network in a 3-dimensional network, given by $z \dashv y \rightarrow x \dashv z$, and let $\omega \in \mathcal{Z}^S$ satisfy

$$l_{y,z} < \theta_{x,y} < u_{y,z}, \quad l_{x,y} < \theta_{z,x} < u_{x,y}, \quad l_{z,x} < \theta_{y,z} < u_{z,x}. \quad (15)$$

Then $\mathcal{F}^S(\omega)$ constructed by the wall-labeling function \mathcal{L}^S (see (15)) is given in Figure 6 on the left. Notice that there does not exist a path from u to u' . Also note that the structure from Figure 5 (left) occurs both on the front face and the back face of the cube in Figure 6 (left). The corresponding $\mathcal{F}^L(\Omega(\omega))$ is shown on the right with a few nodes removed for visual clarity. The bidirectional arrows in Figure 5 (right) correspond to bidirectional arrows in Figure 6 (right) that allow us to find a path from \tilde{u} to \tilde{u}' in $\mathcal{F}^L(\Omega(\omega))$, where $\tilde{u} := \Psi(u)$. \square

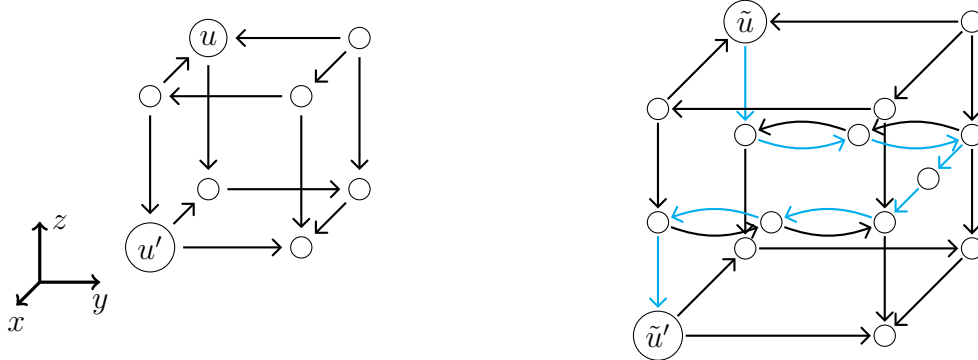


Figure 6: Left: $\mathcal{F}^S(\omega)$, where ω satisfies (15). Notice that there is no path from u to u' . Right: A partial depiction of $\mathcal{F}^L(\Omega(\omega))$, where only some nodes are shown, and $\tilde{u} := \Psi(u)$. A path now exists from \tilde{u} to \tilde{u}' , shown in cyan.

Note that the new path from \tilde{u} to \tilde{u}' in graph of \mathcal{F}^L does not have any effect on the set of Morse sets in the two systems; in both \mathcal{F}^S and \mathcal{F}^L there is unique (attracting) Morse set that consists of the state in the lower right corner of the STG.

To show that the existence of such a path can make a difference in the composition of the set of attractors, we will embed the structure of Figure 6 into a state transition graph for a

four-dimensional network, such that u is part of some attractor $A \in \mathcal{A}^S$ and $u' \notin A$. This will allow us to find a path escaping from the attractor in \mathcal{F}^L .

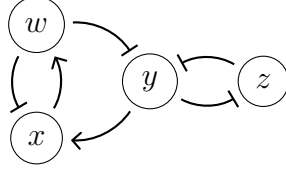


Figure 7: The network that with an S-system given by (16) and parameter satisfying (17) leads to the 4-dimensional attractor in Figure 8.

Lemma 6.3. *Consider the graphs for $\mathcal{F}^S(\omega)$ and $\mathcal{F}^L(\Omega(\omega))$ and an attractor $A \in \mathcal{A}^S$. For $v_i \in A$, there can exist $v_j \notin \mathcal{A}^S$ such that a path from $\Psi(v_i)$ to $\Psi(v_j)$ exists in the graph of \mathcal{F}^L .*

Proof. Consider the network shown in Figure 7. We associate with this network the following equations,

$$\begin{aligned} \dot{x} &= -\gamma_x x + \sigma_{x,y}^+(y) \sigma_{x,w}^-(w) \\ \dot{y} &= -\gamma_y y + \sigma_{y,z}^-(z) \sigma_{y,w}^-(w) \\ \dot{z} &= -\gamma_z z + \sigma_{z,y}^-(y) \\ \dot{w} &= -\gamma_w w + \sigma_{w,x}^+(x) \end{aligned} \tag{16}$$

and consider $\omega \in \mathcal{Z}^S$ satisfying

$$\begin{aligned} l_{x,w} l_{x,y} &< \left\{ \begin{array}{l} u_{x,w} l_{x,y} \\ l_{x,w} u_{x,y} \end{array} \right\} < \theta_{w,x} < u_{x,w} u_{x,y} \\ l_{y,w} l_{y,z} &< l_{y,w} u_{y,z} < \theta_{z,y} < u_{y,w} l_{y,z} < \theta_{x,y} < u_{y,w} u_{y,z} \\ l_{z,y} &< \theta_{y,z} < u_{z,y} \\ l_{w,x} &< \theta_{x,w} < \theta_{y,w} < u_{w,x}. \end{aligned} \tag{17}$$

This parameter leads to the graph of \mathcal{F}^S shown in Figure 8, where the arrows between domains were assigned using the wall-labeling function \mathcal{L}^S with parameter class given by (17). The vertices shown with square shapes are the nodes of a cyclic attractor in \mathcal{F}^S , which can be verified to be an attractor by noting that there are no edges from any square to any circle, and that there is a path from every square node to every other square node. When considering the graph over a canonical map, $\mathcal{F}^L(\Omega(\omega))$, the right half of the top box in Figure 8 (corresponding to the lowest values of w) is identical to Figure 6. Therefore, as in that picture, there is an escape path from $\Psi(u)$ to $\Psi(u')$ in \mathcal{F}^L , even though there is no path from u to u' . Since u in Figure 8 is in the attractor and u' is not, this path demonstrates the lemma. \square

The above proof is based on a network with four nodes. We do not know if such an example exists for $N = 3$, but we suspect it cannot without relaxing the constraints on our logic functions M_j .

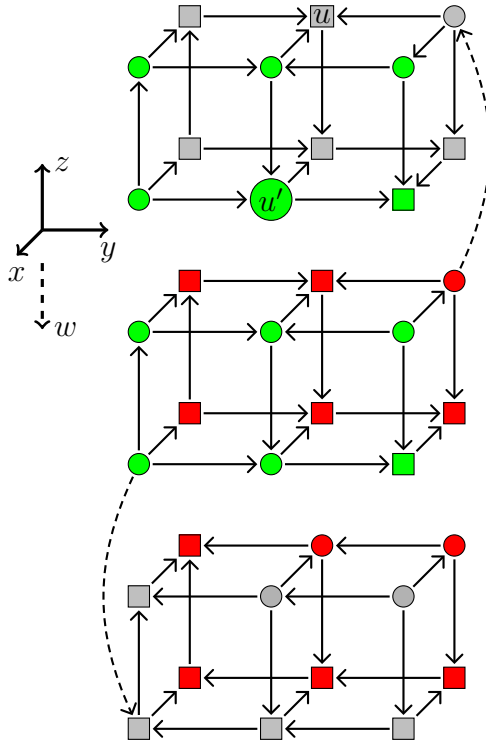


Figure 8: The $\mathcal{F}^S(\omega)$ from Lemma 6.3, with network shown in Figure 7, S-system given by (16), and parameter ω satisfying (17). Nodes in the attractor are depicted as squares, whereas nodes not in the attractor are circles. The color of each node refers to the presence and direction of outgoing edges in the w direction. Green refers to an edge in the $+w$ direction, red refers to an edge in the $-w$ direction, and gray means there is no edge. Two example edges are shown as dashed arrows. The right half of the top box (corresponding to the lowest values of w) is identical to Figure 6, and so an escape path from u to u' exists in $\mathcal{F}^L(\Omega(\omega))$ as it did previously.

Lemma 6.4. *The order-preserving map $\phi : \text{MD}^S \rightarrow \text{MD}^L$ is not necessarily injective.*

Proof. To show this Lemma, it is sufficient to find a network and parameters in which there exist two paths u to u' and u' to u in $\mathcal{F}^L(\Omega(\omega))$, where $\Psi^{-1}(u) \in A$ and $\Psi^{-1}(u') \in B$ for some Morse sets $A, B \in \text{MD}^S$ with $A \neq B$. In this way, two distinct Morse sets in the graph of \mathcal{F}^S will merge into one strongly connected component of \mathcal{F}^L . To do so, we take the previous example network and embed it in a 5-dimensional network, shown in Figure 9 (left), with system of equations given by

$$\begin{aligned}
\dot{x} &= -\gamma_x x + \sigma_{x,y}^+(y) \sigma_{x,w}^-(w) \\
\dot{y} &= -\gamma_y y + \sigma_{y,v}^+(v) \sigma_{y,w}^-(w) \sigma_{y,z}^-(z) \\
\dot{z} &= -\gamma_z z + [\sigma_{z,y}^-(y) + \sigma_{z,v}^+(v)] \\
\dot{w} &= -\gamma_w w + \sigma_{w,v}^-(v) \sigma_{w,x}^+(x) \\
\dot{v} &= -\gamma_v v + \sigma_{v,x}^+(x) \sigma_{v,y}^-(y) \sigma_{v,w}^-(w)
\end{aligned} \tag{18}$$

and $\omega \in \mathcal{Z}^S$ satisfying

$$\begin{aligned}
&\left\{ \begin{array}{l} l_{x,y} l_{x,w} \\ l_{x,y} u_{x,w} \\ u_{x,y} l_{x,w} \end{array} \right\} < \theta_{w,x} < \theta_{v,x} < u_{x,y} u_{x,w} \\
&\left\{ \begin{array}{l} l_{y,v} l_{y,w} l_{y,z} \\ l_{y,v} l_{y,w} u_{y,z} \end{array} \right\} < \theta_{z,y} < l_{y,v} u_{y,w} l_{y,z} < \theta_{v,y} < \theta_{x,y} < \left\{ \begin{array}{l} l_{y,v} u_{y,w} u_{y,z} \\ u_{y,v} u_{y,w} u_{y,z} \\ u_{y,v} l_{y,w} l_{y,z} \\ u_{y,v} l_{y,w} u_{y,z} \\ u_{y,v} u_{y,w} u_{y,z} \end{array} \right\} \\
&l_{z,y} + l_{z,v} < \theta_{y,z} < \left\{ \begin{array}{l} l_{z,y} + u_{z,v} \\ u_{z,y} + l_{z,v} \\ u_{z,y} + u_{z,v} \end{array} \right\} \\
&l_{w,v} l_{w,x} < \left\{ \begin{array}{l} u_{w,v} l_{w,x} \\ l_{w,v} u_{w,x} \end{array} \right\} < \theta_{v,w} < \theta_{x,w} < \theta_{y,w} < u_{w,v} u_{w,x} \\
&l_{v,x} l_{v,y} l_{v,w} < \left\{ \begin{array}{l} l_{v,x} l_{v,y} u_{v,w} \\ l_{v,x} u_{v,y} l_{v,w} \\ u_{v,x} l_{v,y} l_{v,w} \end{array} \right\} < \left\{ \begin{array}{l} l_{v,x} u_{v,y} u_{v,w} \\ u_{v,x} l_{v,y} u_{v,w} \\ u_{v,x} u_{v,y} l_{v,w} \end{array} \right\} < \theta_{w,v} < \theta_{x,v} < \theta_{y,v} < u_{v,x} u_{v,y} u_{v,w}.
\end{aligned} \tag{19}$$

The full state transition graph of $\mathcal{F}^S(\omega)$ is quite extensive, so we offer a schematic as shown in Figure 10, where each square corresponds to a 3-dimensional subset of nodes, each with coordinates x , y , and z . The coordinates v, w are represented in the 2D schematic. The square in cyan is shown in greater detail in Figure 11. Arrows between squares refer to gradient flow in the given direction, so that no paths exist in the direction opposite the arrow between any pair of nodes with the same x, y, z coordinates. The dark blue rectangles labeled XC_1 and XC_2 represent cyclic Morse sets in the S-system composed of a subset of the nodes in the boxes they overlap. XC_2 is an unstable Morse set, because there is a path from a node in XC_2 to XC_1 , which can be seen in Figure 14 in the Appendix where we exhibit the

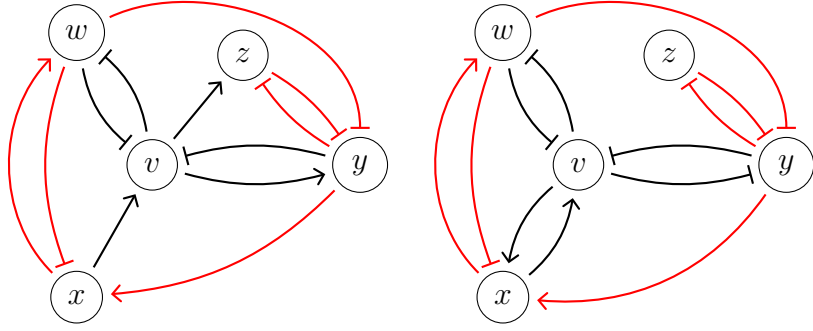


Figure 9: Left: The 5-dimensional network for Lemma 6.4. Right: The 5-dimensional network for Lemma 6.5. In both cases, the embedded 4D network is shown in red.

full state transition graph. The Morse graph MG^S is shown in Figure 10 (right) with only the black arrow.

In $\mathcal{F}^L(\Omega(\omega))$, there is a new path in the cyan box which connects XC_1 to XC_2 , as depicted in Figure 11 and as summarized in the Morse graph for $\mathcal{F}^L(\Omega(\omega))$ shown in Figure 10 (right), dashed cyan arrow. However, no such path exists in $\mathcal{F}^S(\omega)$. The escape path connects a node in the attracting cycle XC_1 to a node from which a path exists to XC_2 . Therefore in the Morse graph of $\mathcal{F}^L(\Omega(\omega))$, the two XC cycles merge into one stable FC cycle. \square

Lemma 6.5. *The order-preserving map $\phi : \mathcal{A}^S \rightarrow \mathcal{A}^L$ restricted only to attractors is, in general, not injective.*

Proof. To show this we modify the network and parameter of the previous Lemma. Consider the network in Figure 9 right. Again, the basic structure of \mathcal{F}^S from Figure 8 will be embedded in XC_1 of the first column in the schematic Figure 12 (left). We will exhibit a path from a node $u \in \mathcal{V}^L$ where $\Psi^{-1}(u) \in A$ for some $A \in \mathcal{A}^S$ to a node $u' \in \mathcal{V}^L$ where $\Psi^{-1}(u') \in B$ for an attractor $B \neq A$. To do so, we endow the network shown in Figure 9 right with an S-system

$$\begin{aligned}
 \dot{x} &= -\gamma_x x + [\sigma_{xy}^+(y) + \sigma_{xv}^+(v)] \sigma_{xw}^-(w) \\
 \dot{y} &= -\gamma_y y + \sigma_{yz}^-(z) \sigma_{yw}^-(w) \sigma_{yv}^-(v) \\
 \dot{z} &= -\gamma_z z + \sigma_{zy}^-(y) \\
 \dot{w} &= -\gamma_w w + \sigma_{wx}^+(x) \sigma_{wv}^-(v) \\
 \dot{v} &= -\gamma_v v + \sigma_{vx}^+(x) \sigma_{vy}^-(y) \sigma_{vw}^-(w)
 \end{aligned} \tag{20}$$

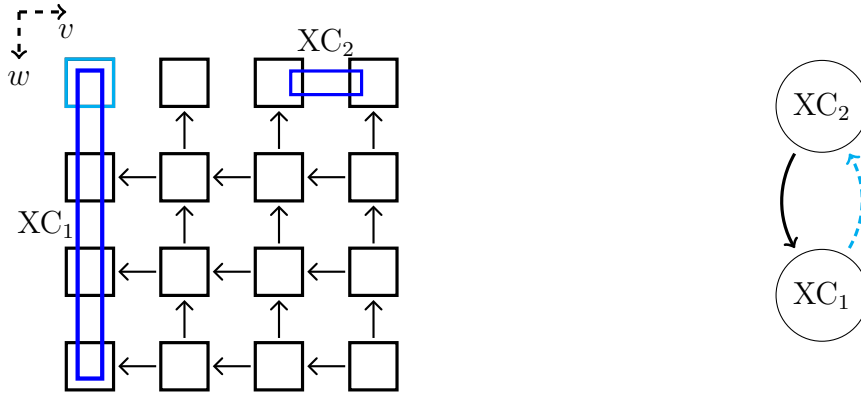


Figure 10: Left: A general schematic of $\mathcal{F}^S(\omega)$ from Lemma 6.4. Each square corresponds to a 3D subset of nodes, with coordinates differing in x , y , and z only. The square in cyan is shown in greater detail in Figure 11. Arrows between squares refer to gradient flow in the given direction, i.e. no paths exist in the direction opposite the arrow. The dark blue rectangles labeled XC_1 and XC_2 represent cyclic Morse sets composed of a subset of the nodes in the boxes they overlap. In $\mathcal{F}^L(\Omega(\omega))$, there is a new path in the cyan box which connects XC_1 to XC_2 . However, no such path exists in $\mathcal{F}^S(\omega)$. The full left column and top row are provided in Figures 13 and 14 (left) respectively. Right: The corresponding (partial) Morse graph. The cyan edge is added only in $\mathcal{F}^L(\Omega(\omega))$, merging XC_1 and XC_2 into one strongly connected component, showing that ϕ , in general, is not injective between the Morse decompositions.

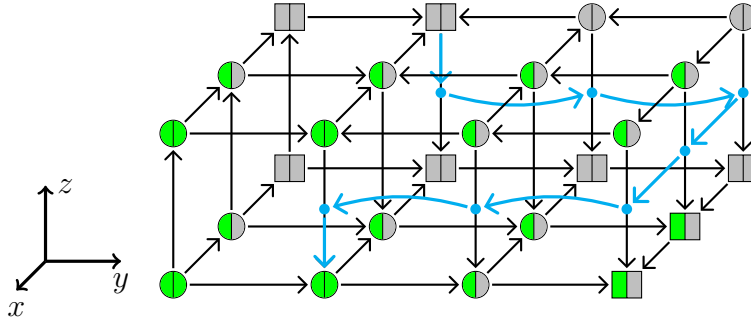


Figure 11: The full set of nodes which correspond to the upper left cyan square in both Figures 10 and 12. Nodes in XC_1 are denoted as squares; all other nodes are circles. The cyan path exists in $\mathcal{F}^L(\Omega(\omega))$ from a node in XC_1 to a node not in it, but still in the 3D set of nodes, represented by the cyan box of Figures 10 and 12. This path makes use of the same structure as the previous examples. The color of each node refers to the outgoing arrows in the v and w directions. The left half of each node corresponds to w and the right half to v . Green means there is an edge from the node to the next corresponding node in the $+$ direction. Gray means no outgoing edge in the corresponding direction. There are no edges in the $-$ direction, since this graph represents the lowest states of the v and w directions.

and we consider any $\omega \in \mathcal{Z}^S$ satisfying

$$(l_{x,y} + l_{x,v})l_{x,w} < \left\{ \begin{array}{l} (u_{x,y} + l_{x,v})l_{x,w} \\ (l_{x,y} + u_{x,v})l_{x,w} \\ (l_{x,y} + l_{x,v})u_{x,w} \\ (l_{x,y} + u_{x,v})u_{x,w} \end{array} \right\} < \theta_{w,x} < \theta_{v,x} < \left\{ \begin{array}{l} (u_{x,y} + l_{x,v})u_{x,w} \\ (u_{x,y} + u_{x,v})l_{x,w} \end{array} \right\} < (u_{x,y} + u_{x,v})u_{x,w} \quad (21)$$

$$l_{y,z}l_{y,w}l_{y,v} < \left\{ \begin{array}{l} u_{y,z}l_{y,w}l_{y,v} \\ l_{y,z}u_{y,w}l_{y,v} \\ l_{y,z}l_{y,w}u_{y,v} \\ u_{y,z}u_{y,w}l_{y,v} \\ u_{y,z}l_{y,w}u_{y,v} \end{array} \right\} < \theta_{z,y} < l_{y,z}u_{y,w}u_{y,v} < \theta_{v,y} < \theta_{x,y} < u_{y,z}u_{y,w}u_{y,v} \quad (22)$$

$$l_{z,y} < \theta_{y,z} < u_{z,y} \quad (23)$$

$$l_{w,v}l_{w,x} < \left\{ \begin{array}{l} u_{w,v}l_{w,x} \\ l_{w,v}u_{w,x} \end{array} \right\} < \theta_{v,w} < \theta_{x,w} < \theta_{y,w} < u_{w,v}u_{w,x} \quad (24)$$

$$l_{v,x}l_{v,y}l_{v,w} < \left\{ \begin{array}{l} l_{v,x}l_{v,y}u_{v,w} \\ l_{v,x}u_{v,y}l_{v,w} \\ u_{v,x}l_{v,y}l_{v,w} \end{array} \right\} < \left\{ \begin{array}{l} l_{v,x}u_{v,y}u_{v,w} \\ u_{v,x}l_{v,y}u_{v,w} \\ u_{v,x}u_{v,y}l_{v,w} \end{array} \right\} < \theta_{w,v} < \theta_{z,v} < \theta_{y,v} < u_{v,x}u_{v,y}u_{v,w}. \quad (25)$$

A schematic of $\mathcal{F}^S(\omega)$ is shown in Figure 12. In the S-system there are two attractors, XC_1 which is the same as in the previous example, and a new attractor, denoted FC. Instead of a path connecting XC_1 to another cycle XC_2 , as in the previous example, there is now a path in $\mathcal{F}^L(\Omega(\omega))$ from XC_1 to a fixed point FP. It follows that in $\mathcal{F}^L(\Omega(\omega))$ the set XC_1 loses stability, and the only attractor is FP. Therefore ϕ cannot be injective even when confined to the set of attractors. \square

Remark 6.6. The complete graphs of $\mathcal{F}^S(\omega)$ and $\mathcal{F}^L(\Omega(\omega))$ of the previous two Lemmas are cumbersome and do not contribute greatly to understanding on a first reading. However, the complete set of nodes corresponding to the left column and top row are included in Figures 13 and 14. We do not include views into other 3D subgraphs, since there is gradient flow between them in v or w directions, and so there are no other stable Morse sets within them.

7 Discussion

Differential equations have been a cornerstone of mathematical modeling of physical systems since the time of Newton. The need for predictive modeling of other continuous time processes without first principle models, like in biology, led to further expansion of these models. However, complex systems of interacting elements consisting of many equations that are often poorly parameterized provides significant challenges to our existing paradigm of analysis of differential equations.

Switching systems (S-systems in this paper) were proposed as a platform for modeling continuous time processes in gene regulation. The underlying assumption of these models is that

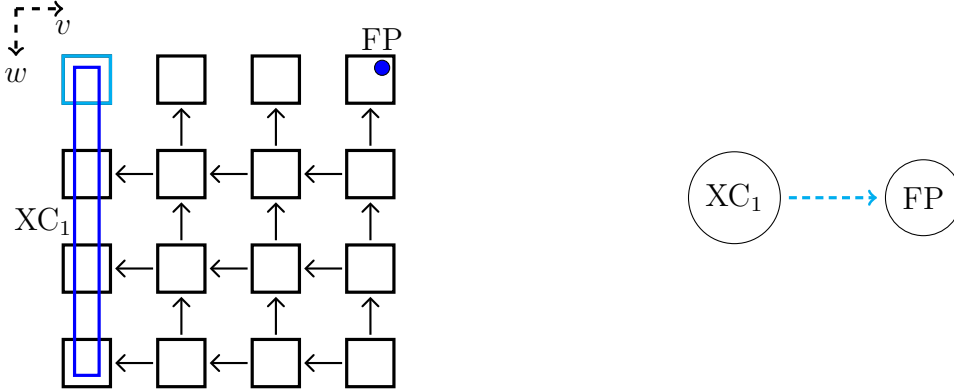


Figure 12: Left: Similar to Figure 10, a general schematic of $\mathcal{F}^S(\omega)$ from Lemma 6.5. Each square corresponds to a 3D subset of nodes, with coordinates differing in x , y , and z only. Arrows between squares refer to gradient flow in the given direction, i.e. no paths exist in the direction opposite the arrow. The square in cyan is shown in greater detail in Figure 11. In $\mathcal{F}^L(\Omega(\omega))$, there is a new path in the cyan box which connects XC_1 to FP . The full left column and top row are provided in Figures 13 and 14 respectively. Right: The corresponding (partial) Morse graph. The cyan edge is added only in $\mathcal{F}^L(\Omega(\omega))$, showing that ϕ cannot be made injective even when constrained to attractors. In effect, XC_1 loses stability in $\mathcal{F}^L(\Omega(\omega))$.

regulatory genetic networks execute a Boolean function, but that this execution is embedded in a continuous flow of time that leads to system of equations with discontinuous right hand sides. There have been many arguments about the appropriateness of such models, the technical challenges they introduce, and, importantly, whether and how these models represent the dynamics of nearby perturbed continuous models [24, 18]. One of the key advantages of the S-systems is that they provide a means to combinatorialize the dynamics of the ODE system in terms of state transition graphs (STGs). These provide incomplete [20, 19, 15] information about the dynamics. In our description this information is captured in a Morse graph [33, 12]. Morse graphs provide information on the number and type of attractors present.

In this paper we define a natural extension of state transition graphs for smooth systems that can be viewed as continuous perturbations (not necessarily small) of the S-systems, where the perturbations are localized in the neighborhoods of thresholds. We call these L-systems. We study the natural question of how the Morse graph of such a perturbation relates to a Morse graph of the S-system for a class of regulatory networks with no negative self-regulation. We show that there is a surjection from the set of attractors in the Morse graph of an S-system to the set of attractors of the L-system, and that this surjection is a bijection on the set of fixed point attractors. Therefore no new stable behavior can be introduced by perturbation to a smooth system. Therefore the S-system contains essential information about attractors of the smooth systems although attractors may be lost or new unstable regions introduced by such a perturbation.

As important as these results are, our constructed examples of systems that show that stronger relationships than those exhibited do not exist. It is easy to construct an example

that shows that an L-system can have more unstable Morse sets than the corresponding S-system. It is a much harder task to construct an L-system which combines two attractors of the S-system into a single attractor of the L-system. As a consequence of these results, one way one could hope to strengthen the results about the correspondence between the Morse graphs of the switching system and its smooth perturbations, represented by the L-system, is to refine a definition of the STG for the L-system. Whether a refinement that would provide a closer correspondence between Morse graphs exists is currently an open question.

A Proof of Theorem 3.8

Proof. Let κ and κ' be two domains with corresponding states $s_1 := g^S(\kappa)$ and $s_2 := g^S(\kappa')$, using the notation of Definition 2.3. Note that the target state of κ is given by

$$t_1 := D^S(s_1) = G^S \circ \Gamma^{-1} \Lambda^S(\kappa),$$

using (10).

First suppose that $s_1 = s_2 = t_1$, as in part (a) of Definition 2.3 of the asynchronous update rule. This is true if and only if $\Gamma^{-1} \Lambda^S(\kappa) \in \kappa$, which is equivalent to κ being an attracting domain, which is exactly part (a) of Definition 3.6.

Now we consider parts (b) of the two definitions. Note that two domains κ and κ' are adjacent if and only if the corresponding states s_1 and s_2 are adjacent. So presume that κ and κ' share a face τ , which means s_1 and s_2 are adjacent. Let $\theta_{j,i} = \pi_i(\tau)$ be the threshold at the face, and assume without loss of generality that τ is a right face of κ and a left face of κ' , so that $\text{sgn}(\tau, \kappa) = -1$, $\text{sgn}(\tau, \kappa') = 1$. By the definition of g^S , this means that $s_{1,i} < s_{2,i}$.

Assume first that $s_2 \in \mathcal{F}^S(s_1)$ so that $\mathcal{L}^S((\tau, \kappa)) = -1$, $\mathcal{L}^S((\tau, \kappa')) = 1$. Since $\text{sgn}(\tau, \kappa) = \mathcal{L}^S((\tau, \kappa)) = -1$ by assumption, we have

$$\begin{aligned} \text{sgn}(\Lambda_i^S(\kappa)/\gamma_i^S - \theta_{j,i}) &= 1 \\ \Rightarrow \Lambda_i^S(\kappa)/\gamma_i^S &> \theta_{j,i} > \pi_i(\text{int } \kappa). \end{aligned}$$

Since $s_{1,i} = \pi_i(g^S(\kappa)) = G_i^S(x_{1,i})$ for arbitrary $x_{1,i} \in \pi_i(\text{int } \kappa)$, we have that

$$s_{1,i} = G_i^S(x_{1,i}) < G_i^S(\Lambda_i^S(\kappa)/\gamma_i^S) = t_{1,i}.$$

The statements $s_{1,i} < s_{2,i}$ and $s_{1,i} < t_{1,i}$ then verify Definition 2.3 (b).1.

In the reverse direction, we have already proved that $s_{1,i} < s_{2,i}$ and $s_{1,i} < t_{1,i}$ imply $\mathcal{L}^S((\tau, \kappa)) = -1$, since all statements were equivalencies. We show that $\mathcal{L}^S((\tau, \kappa')) = 1$ by way of contradiction. Suppose $\mathcal{L}^S((\tau, \kappa')) = -1$. Then

$$\Lambda_i^S(\kappa')/\gamma_i^S < \theta_{j,i},$$

which implies that x_i is increasing below $\theta_{j,i}$ and decreasing above $\theta_{j,i}$. This means that the i -th component of the target point changes between κ_1 and κ_2 , and these domains only differ

in i -th coordinate. This implies that the node i of the network **RN** is regulating itself; the fact that it is negative self-regulation follows from the signs of the vector field in κ and κ' and the fact that $\pi_i(\text{int } \kappa) < \pi_i(\text{int } \kappa')$. Since we assume that **RN** has no negative self-regulation, it must be that $\mathcal{L}^S((\tau, \kappa')) = 1$, as desired.

We have shown that if there are two adjacent domains κ on the left and κ' on the right and $s_2 \in \mathcal{F}^S(s_1)$ according to Definition 3.6 part (b), this is equivalent to condition (b).1 in Definition 2.3. We leave it to the reader to show in a similar fashion that if $s_{2,i} > s_{1,i}$ and $s_{2,i} > t_{2,i}$ (interchanging indices 1 and 2) then the Definition 2.3 (b).2 is equivalent to $s_1 \in \mathcal{F}^S(s_2)$. under the same domain adjacency conditions. \square

B Proof of Theorem 3.14

The main result in this section is Theorem B.2, from which the proof of Theorem 3.14 follows.

For any ℓ -cell $\zeta \in \mathbb{R}^N$, $\zeta = \prod_{i=1}^N [\varphi_i, \varphi'_i]$ with $0 \leq \ell \leq N$ recall from Definition 3.1 that

$$ND(\zeta) := \{j \mid \varphi \neq \varphi'\}$$

is the set of non-degenerate indices, where $|ND(\zeta)| = \ell$. Let $ND^c(\zeta) := \{1, \dots, N\} \setminus ND(\zeta)$ be the complement of $ND(\zeta)$.

Theorem B.1. *Let $z^L \in Z^L$ be a regular parameter for a L -system, and let $\zeta = \prod_{i=1}^N [\varphi_i, \varphi'_i]$ be an ℓ -cell in \mathbb{R}^N with $0 \leq \ell < N$. For $k \in ND(\zeta)$ let $W_k := \zeta \cap \{x_k = \varphi_k\}$ and let $W'_k := \zeta \cap \{x_k = \varphi'_k\}$. In the case where $\varphi'_k = +\infty$, choose an arbitrary point $p_k > \varphi_k$ and set $W'_k := \zeta \cap \{p_k = \varphi'_k\}$. Then for any $j \in ND^c(\zeta)$*

1. $\dot{x}_j > 0$ on $W_k \cup W'_k$ implies $\dot{x}_j > 0$ everywhere in ζ ;
2. $\dot{x}_j < 0$ on $W_k \cup W'_k$ implies $\dot{x}_j < 0$ everywhere in ζ .

Proof. Let ζ be an ℓ -cell with $0 \leq \ell < N$ and let $k \in ND(\zeta)$. Define W_k and W'_k as in the theorem. Let $j \in ND^c(\zeta)$; then $\zeta \subseteq \{x_j = \varphi_j\}$ for some threshold φ_j . Define

$$H_j(x) := \Lambda_j(x) - \gamma_j \varphi_j$$

to be the the right-hand side of the equation for $\dot{x}_j = H_j(x)$ on ζ . Assume that $\text{sgn}(\dot{x}_j)$ is constant and nonzero on $W_k \cup W'_k \subset \zeta$.

Let $q \in \zeta$ be an arbitrary point. Then there exists a scalar $\alpha \geq 0$ such that $u := q - \alpha \vec{e}_k \in W_k$, where \vec{e}_k is the unit vector along the k -th coordinate. Let $h : [0, 1] \rightarrow \zeta$ be the line segment along the k -th coordinate direction that starts in W_k , passes through Q , and ends in W'_k :

$$h(s) = u + s(\varphi'_k - \varphi_k)\vec{e}_k, \quad 0 \leq s \leq 1$$

Note that $h(0) = u \in W_k$ and $h(1) \in W'_k$ and $h(s_1) = Q$ for some $s_1 \in [0, 1]$.

We consider the two cases in which k has either a regulatory effect on j or not. Expressed in terms of edges in the network \mathbf{RN} , this means either (k, j) is an edge in \mathbf{RN} ($(k, j) \in E$) or (k, j) is not an edge in \mathbf{RN} ($(k, j) \notin E$). First consider $(k, j) \notin E$. Then the derivative $\dot{x}_j = H_j(x)$ does not depend on x_k . Since the only variable that changes value along the line segment $h(s)$ is x_k , the derivative $\dot{x}_j(h(s)) = H_j(h(s))$ is constant. Since we know that \dot{x}_j has the same sign everywhere on W_k it must have the same sign along $h(s)$. Since q and thus $h(s)$ was arbitrary, the same is true for any point $y \in \zeta$.

Now consider the case where $(k, j) \in E$. We observe that on $h(s)$, the function Λ_j is a linear function of $\sigma_{j,k}(h(s))$. This occurs because Λ_j is multi-affine in $\sigma_{j,i}$ for all $i \in \mathbf{S}(j)$, the sources of j . But all $x_i \neq x_k$ are constant on $h(s)$, so Λ only changes linearly with respect to $\sigma_{j,k}(h(s))$. We conclude that $H_j(h(s))$ is a linear function in $\sigma_{j,k}(h(s))$.

Recall that $l_{j,k} \leq \sigma_{j,k}(h(s)) \leq u_{j,k}$, and these bounding values are attained at the boundaries $h(s) = \varphi_k$ and $h(s) = \varphi'_k$. Therefore

$$\min\{\sigma_{j,k}(\varphi_k), \sigma_{j,k}(\varphi'_k)\} \leq \sigma_{j,k}(h(s)) \leq \max\{\sigma_{j,k}(\varphi_k), \sigma_{j,k}(\varphi'_k)\}.$$

From this inequality and the linearity of H_j in $\sigma_{j,k}(h(s))$, we conclude

$$\min\{H_j(h(0)), H_j(h(1))\} \leq H_j(h(s)) \leq \max\{H_j(h(0)), H_j(h(1))\}$$

for all $s \in [0, 1]$.

When $\dot{x}_j > 0$ on $W_k \cup W'_k$, then $H_j(h(0)) > 0$ and $H_j(h(1)) > 0$, which implies $H_j(h(s)) > 0$ for $0 \leq s \leq 1$. Likewise, when $\dot{x}_j < 0$ on $W_k \cup W'_k$, then $H_j(h(0)) < 0$ and $H_j(h(1)) < 0$, which implies $H_j(h(s)) < 0$ for $0 \leq s \leq 1$. Since the selection of q and hence $h(s)$ was arbitrary, we have proven that the sign of \dot{x}_j on ζ is determined by its sign on $W_k \cup W'_k$. \square

Theorem B.2. *Let z^L be a regular parameter for an L -system, and let $\zeta := \prod_{i=1}^N [\varphi_i, \varphi'_i]$. be an ℓ -cell in \mathbb{R}^N with $0 \leq \ell < N$. Then for all $j \in ND^c(\zeta)$ we have*

1. $\mathbf{Sign}(\mathcal{C}(\zeta), j) = +1$ implies $\dot{x}_j > 0$ everywhere in ζ ;
2. $\mathbf{Sign}(\mathcal{C}(\zeta), j) = -1$ implies $\dot{x}_j < 0$ everywhere in ζ .

Proof. Suppose $\ell = 0$. Then $\mathcal{C}(\zeta) = \zeta$ and the proof is immediate. This is the base case for an inductive proof. Let ζ be an ℓ -cell with $1 \leq \ell < N$ and assume that for all $(\ell - 1)$ -cells the theorem holds. Let $j \in ND^c(\zeta)$ be a degenerate index.

First assume that $\mathbf{Sign}(\mathcal{C}(\zeta), j) = +1$. Pick any $k \in ND(\zeta)$, let $[\varphi_k, \varphi'_k]$ be the corresponding non-degenerate interval and let $W_k := \zeta \cap \{x_k = \varphi_k\}$, $W'_k := \zeta \cap \{x_k = \varphi'_k\}$. Notice that by Definition 3.1, W_k and W'_k are $(\ell - 1)$ -cells. Furthermore $\mathcal{C}(W_k) \subseteq \mathcal{C}(\zeta)$, and so by Definition 3.10, $\mathbf{Sign}(\mathcal{C}(W_k), j) = +1$. By our inductive hypothesis, $\dot{x}_j > 0$ everywhere in W_k . A similar argument shows that $\dot{x}_j > 0$ everywhere in W'_k as well. Then by Theorem B.1, $\dot{x}_j > 0$ everywhere in ζ .

A similar argument is used when $\mathbf{Sign}(\mathcal{C}(\zeta), j) = -1$. This finishes the induction and hence the proof. \square

C Lemmas for Section 5

In the following, we assume that constructions in the S- and L-systems come from equivalence class parameters ω^S and $\omega^L := \Omega(\omega^S)$.

Definition C.1. We define the bijection

$$\beta = (g^L)^{-1} \circ \Psi \circ g^S : \mathcal{K}^S \rightarrow \mathcal{K}_N^L$$

and the order-preserving functions

$$\begin{aligned} \beta^-(\theta_{j,i}) &= \vartheta_{j,i}^- \\ \beta^+(\theta_{j,i}) &= \vartheta_{j,i}^+. \end{aligned}$$

When $\kappa, \kappa' \in \mathcal{K}^S$ are adjacent with shared face $\tau \subset \{x_i = \theta_{j,i}\}$, consider the domain $\eta \in \mathcal{K}_{N-1}^L$

$$\eta = \prod_{k=1}^{i-1} \beta_k(\kappa) \times [\beta^-(\theta_{j,i}), \beta^+(\theta_{j,i})] \times \prod_{k=i+1}^N \beta_k(\kappa).$$

It is easy to see that

1. η shares a face with $\beta(\kappa)$, $\tau^- := \eta \cap \beta(\kappa) \subset \{x_i = \vartheta_{j,i}^-\}$
2. η shares a face with $\beta(\kappa')$, $\tau^+ := \eta \cap \beta(\kappa') \subset \{x_i = \vartheta_{j,i}^+\}$.

In other words, η is the unique domain that lies between $\beta(\kappa)$ and $\beta(\kappa')$, and this domain is in the subset $\mathcal{K}_{N-1}^L \subset \mathcal{K}^L$.

The next Lemma is the key result from which many results about the correspondence between the Morse graphs follow.

Lemma C.2. Consider $\mathcal{F}^S(\omega^S)$ and of $\mathcal{F}^L(\Omega(\omega^S))$ and two adjacent domains $\kappa, \kappa' \in \mathcal{K}^S$ with shared face $\tau \subset \{x_i = \theta_{j,i}\}$. Let $\zeta := \beta(\kappa)$, $\zeta' := \beta(\kappa')$, $\zeta, \zeta' \in \mathcal{K}_N^L$ be the corresponding domains in \mathcal{K}_N^L and let $\eta \in \mathcal{K}_{N-1}^L$ be the unique domain lying between ζ and ζ' . Let $v := g^S(\kappa)$, $v' := g^S(\kappa')$, $v, v' \in \mathcal{V}^S$, let $w := g^L(\zeta)$, $w' := g^L(\zeta')$, $w, w' \in \mathcal{V}^{SL}$, and $u = g^L(\eta)$. Then $v \rightarrow v' \in \mathcal{F}^S(\omega)$ if and only if $w \rightarrow u \rightarrow w' \in \mathcal{F}^L(\Omega(\omega))$.

Proof. We consider the case when (τ, κ) is the right wall of κ ($\text{sgn}((\tau, \kappa)) = -1$) and (τ, κ') is the left wall of κ' ($\text{sgn}((\tau, \kappa')) = +1$). A similar argument holds in the other case. Then $v' \in \mathcal{F}^S(v)$ if and only if $\mathcal{L}^S((\tau, \kappa)) = -1$ and $\mathcal{L}^S((\tau, \kappa')) = +1$, which by Definition 3.5, implies that

$$\Lambda_i^S(\kappa)/\gamma^S > \theta_{j,i}, \quad \Lambda_i^S(\kappa')/\gamma^S > \theta_{j,i}.$$

By Definition 4.4 of the correspondence Ω we know that $D^S \circ g^S(\kappa) = D_N^L \circ g^L(\zeta)$, so if $\Lambda_i^S(\kappa)/\gamma^S > \theta_{j,i}$, then

$$\Lambda_i^L(\zeta)/\gamma_i^L > \beta^+(\theta_{j,i}) \quad \Lambda_i^L(\zeta')/\gamma_i^L > \beta^+(\theta_{j,i}).$$

Then from Definition 3.10 we get $\mathbf{Sign}(\mathcal{C}(\tau^-), i) = \mathbf{Sign}(\mathcal{C}(\tau^+), i) = +1$. We note that τ^- is a right face of ζ and a left face of η , while τ^+ is a right face of η and a left face of ζ' , by the assumptions of the Lemma. With this information we can compute

$$\begin{aligned}\mathcal{L}^L((\tau^-, \zeta)) &= -1 \cdot +1 = -1, & \mathcal{L}^L((\tau^-, \eta)) &= +1 \cdot +1 = +1 \\ \mathcal{L}^L((\tau^+, \eta)) &= -1 \cdot +1 = -1, & \mathcal{L}^L((\tau^+, \zeta')) &= +1 \cdot +1 = +1.\end{aligned}$$

Finally, by Definition 3.10 this is equivalent with the existence of a path $w \rightarrow u \rightarrow w'$ in \mathcal{V}^L . Since all the previous statements are equivalencies this finishes the proof. \square

Corollary C.3. *Consider $\mathcal{F}^S(\omega^S)$ and of $\mathcal{F}^L(\Omega(\omega^S))$. For any two $v, v' \in \mathcal{V}^S$ let $w := \Psi(v), w' := \Psi(v')$. Then $v' \in (\mathcal{F}^S)^k(v)$ for some integer k (which means there is a path of length k in the graph $(\mathcal{V}^S, \mathcal{E}^S)$), if and only if $w' \in (\mathcal{F}^L)^{2k}(w)$, where every domain $\kappa_i = (g^L)^{-1}(w_i)$ belongs to $\mathcal{K}_N^L \cup \mathcal{K}_{N-1}^L$ for all nodes w_i in the path.*

Lemma C.4. *Consider a regulatory network \mathbf{RN} , an L -system with regular parameter $z^L \in Z^L$, the set of domains \mathcal{K}^L and nearest neighbor multi-valued map \mathcal{F}^L . Let $\kappa \in \mathcal{K}^L \setminus \mathcal{K}_N^L$ be a domain and let $u = g^L(\kappa)$ have k non-integer components. Then there is a state $v \in \mathcal{V}^L$ with $k - 1$ non-integer components, such that*

$$v \in \mathcal{F}^L(u).$$

Proof. Let $\kappa \in \mathcal{K}^L \setminus \mathcal{K}_N^L$ with $u = g^L(\kappa)$. Then there is an index i such that $\pi_i(\kappa) = [\vartheta_{j,i}^-, \vartheta_{j,i}^+]$. Let τ^- and τ^+ be the left and right faces of κ with projection index i and so $\tau^- \subseteq \{x_i = \vartheta_{j,i}^-\}$ and $\tau^+ \subseteq \{x_i = \vartheta_{j,i}^+\}$. Note that there are two domains η^-, η^+ that are immediate neighbors of κ along the i -th coordinate which satisfy

$$\pi_i(\eta^-) = [\vartheta_{j-1,i}^+, \vartheta_{j,i}^-] \quad \pi_i(\eta^+) = [\vartheta_{j,i}^+, \vartheta_{j+1,i}^-].$$

It follows that the states

$$v^- := g^L(\eta^-) \text{ and } v^+ := g^L(\eta^+).$$

have one more integer value than u .

Let $\mathcal{C}(\tau^-)$ be a collection of corner points of τ^- and $\mathcal{C}(\tau^+)$ be a collection of corner points of τ^+ . Note that there is a bijection α between these two sets and the corresponding corner points that only differ in the i -th values where $\vartheta_{j,i}^-$ is replaced by $\vartheta_{j,i}^+$. Take $q \in \mathcal{C}(\tau^-)$ and assume first that $\mathbf{Sign}(q, i) = +1$. This implies that $\Lambda_i^L(q)/\gamma_i^L > \vartheta_{j,i}^-$. But since at any regular parameter z^L the value

$$\Lambda_i^L(q)/\gamma_i^L \notin [\vartheta_{j,i}^-, \vartheta_{j,i}^+]$$

for any j , we conclude that also $\Lambda_i^L(q)/\gamma_i^L > \vartheta_{j,i}^+$. This in turn implies that at the corner point $\alpha(q) \in \mathcal{C}(\tau^+)$ we have $\mathbf{Sign}(\alpha(q), i) = +1$. We have shown that

$$\mathbf{Sign}(q, i) = +1 \quad \text{if and only if} \quad \mathbf{Sign}(\alpha(q), i) = +1.$$

A similar argument shows that $\mathbf{Sign}(q, i) = -1$ if and only if $\mathbf{Sign}(\alpha(q), i) = -1$ as well. Let $u = g^L(\kappa)$. From the definition of the map \mathcal{F}^L we have

- if there exists at least one corner point $q \in \mathcal{C}(\tau^-)$ with $\text{Sign}(q, i) = -1$, then

$$v^- \in \mathcal{F}^L(u);$$

- if there exists at least one corner point $q \in \mathcal{C}(\tau^+)$ with $\text{Sign}(q, i) = +1$, then

$$v^+ \in \mathcal{F}^L(u).$$

Since the **Sign** of a single corner point can never be zero by the regularity of z^L , we conclude that either one or both of the cases hold. \square

D State transition graphs for the 5D examples

We now present full information about the paths in the proofs of Lemmas 6.4 and 6.5. The first column (Figure 13) and the first rows (Figure 14) of the schematics in Figures 10 and 12 are shown below. The rows have been rotated into columns to make them more legible, and are arranged for side-by-side comparison.

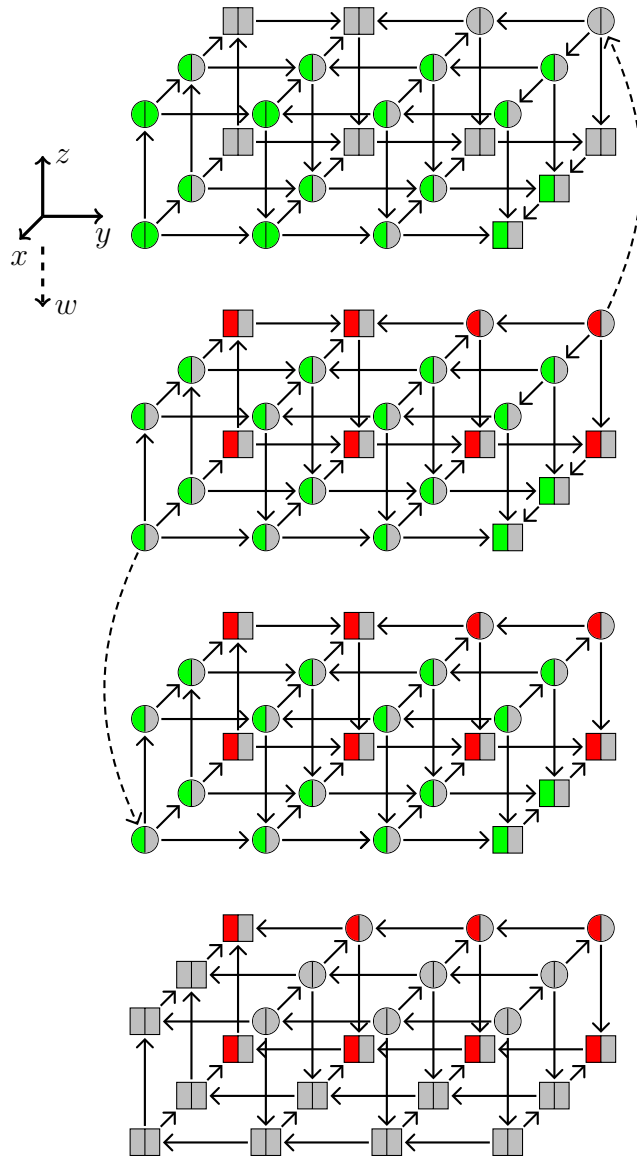


Figure 13: The left column of both Figures 10 and 12. Our choice of networks and parameters allows us to use the same structure in \mathcal{F}^S for the nodes corresponding to the lowest values of v (the top cuboid). The color of each node refers to the outgoing arrows in the v and w directions. The left half of each node corresponds to w and the right half to v . Green means there is an edge from the node to the next corresponding node in the $+$ direction, and red means there is an edge in the $-$ direction. Gray means no outgoing edge in the corresponding direction. Two example dashed arrows are shown. Nodes in XC_1 are shown as squares; all other nodes are shown as circles. The top box is the same one shown in Figure 11.

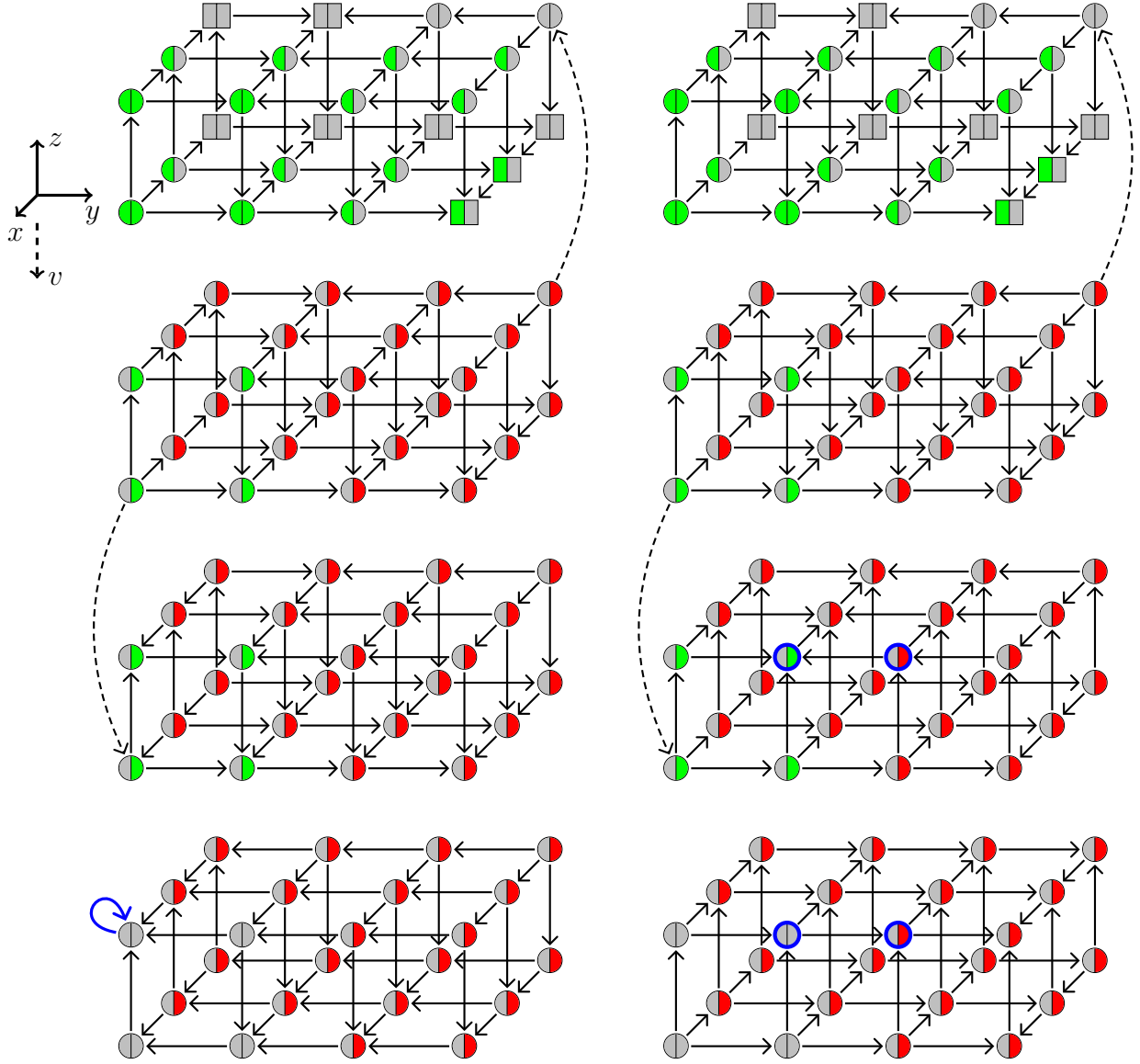


Figure 14: Left: the complete set of all nodes represented by the top row of Figure 12, i.e. the nodes with lowest values of w . The FP is shown as a node with a blue self-loop in the lower left. The top box is a repeat of Figure 11. The same color scheme is used as in Figure 13. Example edges are shown as dotted arrows. Right: the nodes with lowest values of w from Figure 10. XC_2 is shown as the four nodes with dark blue outlines.

Acknowledgements: T. G. was partially supported by NSF grants DMS-1226213, DMS-1361240, USDA 2015-51106-23970, DARPA grants D12AP200025 and FA8750-17-C-0054, and NIH grants 1R01AG040020-01 and 1R01GM126555-01. B.C. was partially supported by grants USDA 2015-51106-23970, DARPA grants D12AP200025 and FA8750-17-C-0054 and NIH 1R01GM126555-01. P. C-K. was supported by USP and INBRE student research grants at Montana State University. Research reported in this publication was supported by the National Institute of General Medical Sciences of the National Institutes of Health under Award Number P20GM103474. The content is solely the responsibility of the authors and does not necessarily represent the official views of the National Institutes of Health.

References

- [1] Reka Albert, James J. Collins, and Leon Glass. Introduction to Focus Issue: Quantitative approaches to genetic networks. Chaos, 23(2):025001, JUN 2013.
- [2] U. Alon. An introduction to systems biology. Chapman & Hall/CRC, 2007.
- [3] Yael Artzy-Randrup, Sarel Fleishman, Nir Ben-Tal, and Lewi Stone. Comment on network motifs: Simple building blocks of complex networks and superfamilies of evolved and designed networks. Science, 305:1107c, 2004.
- [4] G Batt, C. Belta, and R. Weiss. Model checking genetic regulatory networks with parameter uncertainty. In Hybrid Systems: Computation and Control, HSCC07, Lecture Notes in Computer Science 4416, pages 61–75. Springer, Berlin, 2007.
- [5] G Batt, D Ropers, H de Jong, J Geiselmann, R Mateescu, M Page, and D Schneider. Validation of qualitative models of genetic regulatory networks by model checking: analysis of the nutritional stress response in escherichia coli. Bioinformatics, 21(Suppl 1):i19–28, 2005.
- [6] G. Batt, B. Yordanov, R. Weiss, and C. Belta. Robustness analysis and tuning of synthetic gene networks. Bioinformatics, 23(18):2415–2422, 2007.
- [7] C. Belta and L.C.G.J.M. Habets. Controlling a class of nonlinear systems on rectangles. Trabs. Aut. Control, 51:17491759, 2006.
- [8] O Bernard and J Gouze. Global qualitative description of a class of nonlinear dynamical systems. Artificial Intelligence, 136:29–59, 2002.
- [9] DL Burkhardt and J Sage. Cellular mechanisms of tumour suppression by the retinoblastoma gene. Nat Rev Cancer, 8(9):671–82, 2008.
- [10] M Chaves, E D Sontag, and R Albert. Methods of robustness analysis for Boolean models of gene control networks. IEE Proceedings-Systems Biology, 153(4):154–167, 2006.
- [11] M Chinnam and DW Goodrich. RB1, development, and cancer. Curr Top Dev Biol, 94:129–69, 2011.

- [12] B. Cummins, T. Gedeon, S. Harker, K. Mischaikow, and K. Mok. Combinatorial Representation of Parameter Space for Switching Systems. SIAM J. Appl. Dyn. Syst., 15(4):2176–2212, 2016.
- [13] Bree Cummins, Tomas Gedeon, Shaun Harker, and Konstantin Mischaikow. Model rejection and parameter reduction via time series. arXiv, 1706.04234:<http://arxiv.org/abs/1706.04234>, 2017.
- [14] H de Jong, JL Gouze, C Hernandez, M Page, T Sari, and J Geiselmann. Qualitative simulation of genetic regulatory networks using piecewise-linear models. Bull Math Biol, 66(2):301–40, 2004.
- [15] R. Edwards. Chaos in neural and gene networks with hard switching. Diff. Eq. Dyn. Sys., (9):187–220, 2001.
- [16] R. Edwards, a. Machina, G. McGregor, and P. van den Driessche. A Modelling Framework for Gene Regulatory Networks Including Transcription and Translation. Bulletin of Mathematical Biology, pages 953–983, 2015.
- [17] A Faure, A Naldi, C Chaouiya, , and D Thieffry. Dynamical analysis of a generic boolean model for the control of the mammalian cell cycle. Bioinformatics, 22(14):e124e131, 2006.
- [18] Tomas Gedeon, Shaun Harker, Hiroshi Kokubu, Konstantin Mischaikow, and Hiroe Oka. Global dynamics for steep sigmoidal nonlinearities in two dimensions. Physica D, 339:18–38, 2017.
- [19] L Glass and S a Kauffman. Co-operative components, spatial localization and oscillatory cellular dynamics. Journal of Theoretical Biology, 34(2):219–37, February 1972.
- [20] L Glass and S a Kauffman. The logical analysis of continuous, non-linear biochemical control networks. Journal of Theoretical Biology, 39(1):103–29, April 1973.
- [21] AG Gonzalez, A Naldi, L Sanchez, D Thieffry, , and C Chaouiya. Ginsim: a software suite for the qualitative modelling, simulation and analysis of regulatory networks. BioSystems, 84(2):91–100, 2006.
- [22] Zane Huttinga, Bree Cummins, Tomáš Gedeon, and Konstantin Mischaikow. Global dynamics for switching systems and their extensions by linear differential equations. Physica D: Nonlinear Phenomena, 2017.
- [23] Piers J Ingram, Michael Stumpf, and Jaroslav Stark. Network motifs: structure does not determine function. BMC Genomics, 7(108), 2006.
- [24] Liliana Ironi, Luigi Panzeri, Erik Plahte, and Valeria Simoncini. Dynamics of actively regulated gene networks. Physica D: Nonlinear Phenomena, 240(8):779–794, apr 2011.
- [25] G Karlebach and R Shamir. Modelling and analysis of gene regulatory networks. Nature, 9(770), 2008.
- [26] Wenzhe Ma, Ala Trusina, Hana El-Samad, Wendel A. Lim, and Chao Tang. Defining network topologies that can achieve biochemical adaptation. Cell, 138(4):760–773, 2009.

- [27] AL Manning and NJ Dyson. RB: mitotic implications of a tumour suppressor. Nat Rev Cancer, 12(3):220–6, 2012.
- [28] Sarkar CA Shah NA. Robust network topologies for generating switch-like cellular responses. PLoS Comput Biol, 7(6):e1002085, 2011.
- [29] Steven N Steinway, Matthew B Biggs, Thomas P Loughran, Jason A Papin, and Réka Albert. Inference of Network Dynamics and Metabolic Interactions in the Gut Microbiome. PLOS Comput Biol, 11(6):e1004338, June 2015.
- [30] R Thomas. Boolean formalization of genetic control circuits. Journal of Theoretical Biology, 42:563–585, 1973.
- [31] R Thomas. Regulatory networks seen as asynchronous automata: A logical description. Journal of Theoretical Biology, 153:1–23, 1991.
- [32] R Thomas, D Thieffry, and M Kaufman. Dynamical behaviour of biological regulatory networks-i. biological role of feedback loops and practical use of the concept of the loop-characteristic state. Bull Math Biol, 57(2):247–76, 1995.
- [33] Laurent Tournier and Madalena Chaves. Uncovering operational interactions in genetic networks using asynchronous boolean dynamics. J Theor Biol, 260(2):196–209, 2009.